Multi-dimensional Expansion Bases

In chapter 2 we introduced the standard Galerkin technique for spectral/hp element discretisation in one-dimension. Using this construction we illustrated how a global C^0 continuous expansion could be decomposed into either a modal or nodal expansion within a element domain in a standard region. We begin extending this concept to multiple dimensions in this chapter by discussing spectral/hp element multi-dimensional expansions in different standard regions. In chapter 4 we extend the one-dimensional discussion from chapter 2 on elemental operations such as integration and differentiation to multi-dimensions, and also discuss the construction of a global expansion from the local expansions defined in this chapter.

Although the extension to multi-dimensions is analogous to the one-dimensional case, the aim of this chapter is to explain the reasons for the different choices of expansion bases as well as discussing their numerical implementation. All the expansions discussed in this chapter will be considered within a standard region Ω_{st} . In two- or three-dimensions, we now have a choice of different standard regions. In two-dimensions we will consider standard regions that are either a quadrilateral or a triangle. In three-dimensions we will consider standard regions that are either a hexahedron, prism, pyramid, or tetrahedron, which collectively we refer to as hybrid domains. Since we will only be referring to these standard regions we shall not use the superscript e to denote the elemental domain within this chapter. The assembly of these expansions in multiple domains and the treatment of integration and differentiation is discussed in chapter 4.

For tensorial bases we shall denote the polynomial bases by $\phi_{pq}(\xi_1,\xi_2)$ or $\phi_{pqr}(\xi_1,\xi_2,\xi_3)$ in two- or three-dimensions, respectively, where ξ_1,ξ_2,ξ_3 are the standard Cartesian coordinates. This notation may equally well refer to a modal or nodal expansion within a triangular, quadrilateral, or any of the three-dimensional standard regions. Although there is a wide variety of expansion bases, particularly for the standard h-type finite element method, we shall be restricting our attention to those most commonly used in the spectral/hp element literature. The majority of the bases to be discussed can be expressed in terms of a product of one-dimensional functions or tensor product, for example,

$$\phi_{pq}(\xi_1, \xi_2) = \psi_p^a(\xi_1) \psi_q^a(\xi_2),$$

or

$$\phi_{pq}(\xi_1, \xi_2) = h_p(\xi_1)h_q(\xi_2).$$

Expansions which can be constructed with this form allow many numerical operations to be performed very efficiently using the sum factorisation or tensor product techniques discussed in section 4.1.6.

Although most quadrilateral hexahedral expansions are typically constructed from a product of functions, this is not so common for expansions in triangular and tetrahedral domains. In section 3.1 we give a comprehensive discussion of the tensorial extension for all hybrid regions and also introduce the underlying concepts which will be helpful when constructing a tensorial basis for the unstructured region as covered in section 3.1.1. Finally, in section 2.3.4 we discuss non-tensorial, nodal bases in the triangular regions which are compatible with the standard nodal, tensor-based quadrilateral basis.

From a purely implementation point of view, the following details may be of interest. The most commonly used spectral/hp element bases are those which can be expanded into a globally C^0 continuous expansion. The standard tensor product expansions for modal and nodal bases in quadrilateral and hexahedral domains are defined in 3.1. The decomposition of these expansions into an interior and boundary decomposition is discussed in section 3.1.1.2. For the hybrid domains, that is triangular and quadrilateral regions in two-dimensions and tetrahedral, pyramidic, prismatic and hexahedral domains in three-dimensions, a unified C^0 continuous generalised tensorial expansion is defined in sections 3.2.3.1 and 3.2.3.2, and a full listing is also provided in appendix D. This expansion makes use of the collapsed coordinate system discussed in sections 3.2.1.1 and 3.2.1.2, and the assembly of these expansions is detailed in section 3.2.3.3. Finally, two non-tensorial nodal sets of points in a triangular region, compatible with the nodal quadrilateral expansion, are introduced and defined in sections 3.3.3 and 3.3.4 as well as appendix D. For a discontinuous Galerkin formulation it is sometimes convenient to use orthogonal expansions in preference to the modified globally C^0 continuous, expansion. Tensor-based orthogonal expansions in all two- and three-dimensional hybrid regions are defined in section 3.2.2.1, which also uses the collapsed coordinate systems discussed in sections 3.2.1.1 and 3.2.1.2.

Nomenclature

Although already specified in the general nomenclature section, we highlight again here in table 3.1 some of the new notation adopted in this chapter. Similarly to chapter 2 we will use ξ to denote the standard Cartesian directions with a subscript to identify different orthogonal directions depending on the dimension of the basis. Also, following the convention of chapter 2 we will denote any general polynomial expansion as $\phi_{pq}(\xi_1, \xi_2)$ or $\phi_{pqr}(\xi_1, \xi_2, \xi_3)$ in two- or three-dimensions, respectively. The indices p, q and r denote the different components of the tensorial expansion, which is introduced in 3.1. Two commonly used tensorial expansion bases, already introduced in 2.3.3.3 and 2.3.4.2, are the modal modified basis, $\psi_p^a(\eta)$, and the nodal Lagrange basis, $h_p(\xi)$.

To define a generalised tensorial expansion in simplex domains, such as triangles and tetrahedrons, it will be necessary to introduce a new, non-orthogonal Implementation note: Layout of the chapter from the implementation point of

$\boldsymbol{\xi} = (\xi_1, \xi_2, \xi_3)$	Local Cartesian coordinates.	
$\eta_1,\overline{\eta_1},\eta_2,\eta_3$	Local collapsed coordinates.	
$\phi_{pq}(\xi_1, \xi_2)$ $\phi_{pqr}(\xi_1, \xi_2, \xi_3)$	General expansion basis for any $2D$ region General expansion basis for any $3D$ region	
$\begin{array}{l} \psi_p^a(\eta_1), \psi_{pq}^b(\eta_2), \psi_{pqr}^c(\eta_3) \\ \widetilde{\psi}_p^a(\eta_1), \widetilde{\psi}_{pq}^b(\eta_2), \widetilde{\psi}_{pqr}^c(\eta_3) \end{array}$	Modified principal functions Orthogonal principal functions	
$h_p(\xi) \ L_i^{N_m}(oldsymbol{\xi})$	1D Lagrange polynomial of order p 2D Lagrange polynomial though N_m points $\pmb{\xi}_i$	
P_i	Polynomial order in the i -th direction	

Table 3.1 Notation for expansion bases.

coordinate system. We will refer to this new coordinate system as collapsed coordinates and denote each ordinate as η_1, η_2 or η_3 . The collapsed coordinate $\overline{\eta_1}$ will also be used in the pyramidic expansion bases. Its definition is analogous to η_2 . Consistent with the introduction of the collapsed coordinates we will introduce two generalised tensor bases for both a modified, C^0 continuous, basis $\psi^b_{pq}(\eta_2), \psi^c_{pqr}(\eta_3)$ and an orthogonal basis $\widetilde{\psi}^b_{pq}(\eta_2), \widetilde{\psi}^c_{pqr}(\eta_3)$.

In section 2.3.4 we will discuss non-tensorial bases in triangular regions. Since there is no tensorial basis it is more convenient to use the basis notation with a single index for example $\phi_i(\boldsymbol{\xi})$ where $\boldsymbol{\xi} = (\xi_1, \xi_2)$. We, however, understand the index i to sum over all of the two-dimensional modes. We shall also adopt the notation $L_i^{N_m}(\boldsymbol{\xi})$ to denote the multi-dimensional Lagrange polynomial through N_m nodal points $\boldsymbol{\xi}_i$.

Since for multi-dimensional bases the polynomial order can change in each Cartesian direction we shall also adopt the notation P_i where the subscript denotes the i-th Cartesian direction.

3.1 Quadrilateral and Hexahedral Tensor Product Expansions

The extension to higher dimensions within quadrilateral or hexahedral regions is relatively straightforward, if rather more involved than the one-dimensional case discussed in section 2.3.

We start by defining the two-dimensional standard region, Q^2 , as the bi-unit square,

$$\Omega_{st} = \mathcal{Q}^2 = \{-1 \le \xi_1, \xi_2 \le 1\},\$$

and the three-dimensional standard region, Q^3 as the bi-unit cuboid

$$\Omega_{st} = \mathcal{Q}^3 = \{-1 \le \xi_1, \xi_2, \xi_3 \le 1\}.$$

In general, these regions will be referred to as Ω_{st} , which encompasses both Q^2 and Q^3 . Since these regions are trivially defined by a standard Cartesian

coordinate system, the most natural and straightforward way to construct the basis is by taking a product of the one-dimensional basis which can be thought of as one-dimensional tensors. This type of extension may be applied equally well to either the modal- or nodal-type basis, and therefore we shall not distinguish between these two forms except where it is necessary or helpful.

3.1.1 Standard Tensor Product Extensions

In section 2.3.2.1 we introduced a variety of one-dimensional p-type expansion bases which we generally referred to as $\phi_p(\xi)$. Three of the most useful expansions are:

$$\phi_p(\xi) = \begin{cases} \psi_0^a(\xi) = \left(\frac{1-\xi}{2}\right) & p = 0 \\ \psi_p^a(\xi) = \left(\frac{1-\xi}{2}\right)\left(\frac{1+\xi}{2}\right)P_{p-1}^{1,1}(\xi) & 0
$$(3.1)$$$$

$$\frac{\text{Nodal }(C^0 \text{ continuous}) \text{ basis}}{\phi_p(\xi) = h_p(\xi) = \frac{(\xi - 1)(\xi + 1)L'_P(\xi)}{P(P+1)L_P(\xi_p)(\xi - \xi_p)}} \qquad 0 \le p \le P,$$
(3.2)

$$\phi_p(\xi) = \widetilde{\psi}_p^a(\xi) = L_p(\xi). \tag{3.3}$$

The use of definition (3.1) for $\phi_p(\xi)$ corresponds to the C^0 continuous hierarchical modal expansion and is the most commonly used hp-finite element expansion in quadrilateral domains. The original hierarchical expansions for p-type extensions bases were constructed by Peano [366]. This basis was then modified by using the integral of the Legendre polynomial to arrive at the widely adopted form given in equation (3.1) (see Oden [340], and Szabo and Babuška [442]). Note that the integral of the Legendre polynomial is directly related to the $P_n^{1,1}(z)$ Jacobi polynomial as seen from equation (A.9) in appendix A.

Definition (3.2) corresponds to the spectral element nodal basis originally developed using Chebychev expansions by Patera [360]. Definition (3.3) is the Legendre polynomial which is orthogonal in the L^2 or Legendre inner product.

In all these cases the expansion was denoted by a single subscript, p, and so may be considered as a one-dimensional "tensor." The two- and three-dimensional bases can be constructed by a simple product of the one-dimensional tensors in each of the Cartesian coordinate directions, that is,

$$\begin{split} \phi_{pq}(\xi_1,\xi_2) &= \phi_p(\xi_1)\phi_q(\xi_2) & 0 \leq p,q; \ p \leq P_1, q \leq P_2 \\ \phi_{pqr}(\xi_1,\xi_2,\xi_3) &= \phi_p(\xi_1)\phi_q(\xi_2)\phi_r(\xi_3) & 0 \leq p,q,r; \ p \leq P_1, q \leq P_2, r \leq P_3. \end{split}$$

Formulation

note: Most commonly $used\ modal\ polynomial$ $expansion\ basis.$

Formulation

note: Most commonly used nodal polynomial expansion basis.

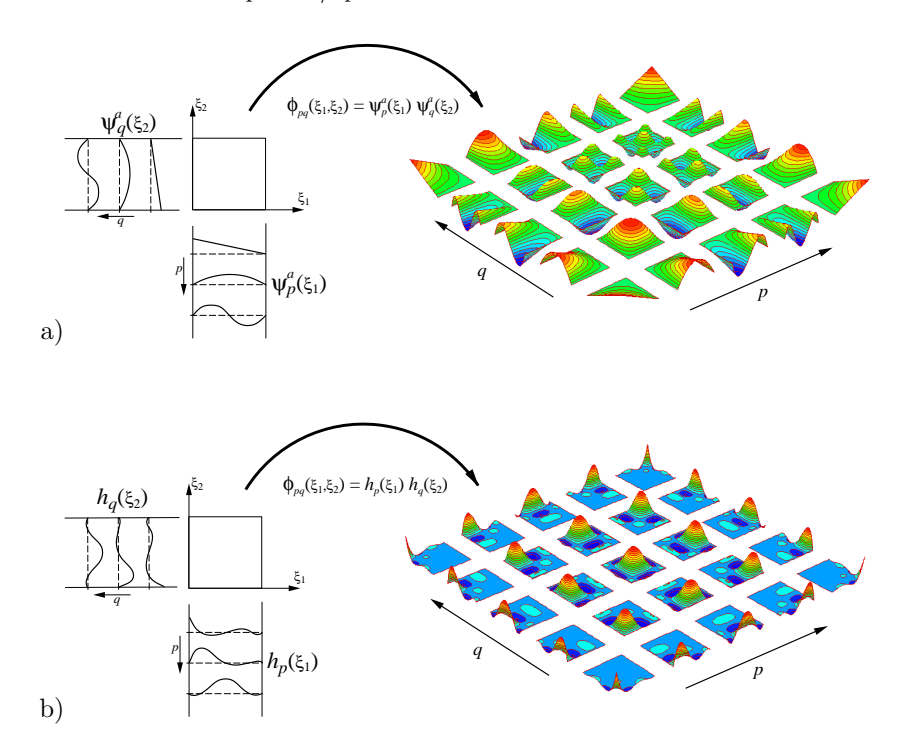


Figure 3.1 Construction of a two-dimensional expansion basis from the product of two one-dimensional expansions of order P=4. (a) Modal expansions using the one-dimensional expansion defined in (3.1) (edge and face modes have been scaled by a factor of 4 and 16 respectively). (b) Nodal expansion using the one-dimensional Lagrange polynomial defined in (3.2).

We note that the polynomial order of the multi-dimensional expansions may differ in each coordinate direction as denoted by the use of the bounds P_1 , P_2 , and P_3 .

Figure 3.1 shows a diagrammatic representation of the tensor product extension to generate a two-dimensional expansion in the standard quadrilateral region using both the modal and nodal one-dimensional expansions. The modal basis shown in figures 3.1(a) was generated using the one-dimensional expansion $\phi_p(\xi) = \psi_p^a(\xi)$ [see equation (3.1)] and the nodal basis expansion shown in figure 3.1(b) was generated using the one-dimensional expansion $\phi_p(\xi) = h_p(\xi)$ [see equation (3.2)]. The expansion modes shown in figure 3.1 represent a complete bi-linear expansion for fourth-order polynomials in both the ξ_1 and ξ_2 directions. Note that the modal expansion maintains a hierarchic form where the lower order expansions are a subset of the higher order expansions. In contrast, each component of the two-dimensional nodal expansion maintains the Kronecker delta form of the Lagrange polynomial where each mode has a unit value at a specified position within the region.

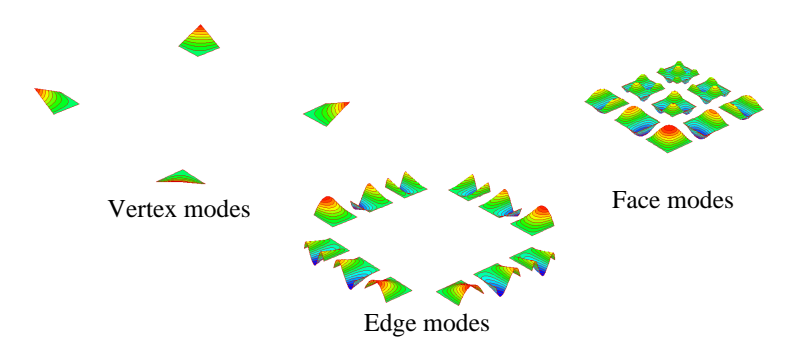


Figure 3.2 Boundary/interior decomposition of the modal expansion shown in figure 3.1(a). The two-dimensional expansion is decomposed into boundary modes (vertex and edge modes) which have support along the boundary of the region, and interior modes which have zero support on all boundaries.

3.1.1.1 Boundary/Interior Decomposition

A significant property of the modal expansion based on definition (3.1) and the nodal expansion based on definition (3.2) is their inherent decomposition into boundary and interior modes. Boundary modes are defined as all the modes which have non-zero support on the boundary of the standard region; interior modes are all the modes which are zero on all boundaries. We recall from section 2.3.2.2 that this type of decomposition is particularly convenient when a C^0 global expansion base is required since a global expansion can be generated from the local expansion simply by matching the shape of individual boundary modes.

An illustration of the decomposition is shown in figure 3.2, where we see all the modes shown in figure 3.1(a) decomposed into vertex, edge, and face modes. We define vertex modes as all modes which have a unit magnitude at one vertex and are zero at all other vertices; edge modes as all modes which have support along one edge and are zero at all other edges and vertices; and face modes as all modes which have magnitude along one face but are zero along all other faces, edges, and vertices. For a two-dimensional expansion the boundary modes are made up of the vertex and edge modes whereas in three-dimensions the boundary decomposition contains the vertex, edge, and face modes. The face modes of the three-dimensional expansions are analogous to the interior modes of the two-dimensional expansion. It should be appreciated that an identical decomposition is possible for the nodal basis shown in figure 3.1(b) under the definitions presented above. We further note that the vertex modes of the modal expansion are identical to the standard linear finite element basis for a quadrilateral sub-domain.

3.1.1.2 Construction Procedure for the Local Expansion

The definition of the two- and three-dimensional expansion bases ϕ_{pq} and ϕ_{pqr} as a tensor product of the one-dimensional functions defined in equations (3.1) and (3.2) enables the boundary and interior modes to be interpreted intuitively

as discussed in the following sections.

Implementation

note: Definition of Boundary and Interior modes for 2D Tensor product expansions.

Two-Dimensional Expansion

If we consider the two-dimensional basis, $\phi_{pq}(\xi_1, \xi_2)$, as a two-dimensional array spanning a similar region as the standard quadrilateral illustrated in figure 3.3(a), then the indices of the boundary modes correspond to their location within this array. For example, the vertex mode which has magnitude at the corner of the quadrilateral marked A corresponds to the indices p=0, q=0 and so $\phi_{0,0}(\xi_1,\xi_2)=\psi_0^a(\xi_1)\psi_0^a(\xi_2)$ is the appropriate mode for this vertex of a modal expansion. The vertex mode at p=0, q=0 in the previously defined nodal expansion is $\phi_{0,0}(\xi_1,\xi_2)=h_0(\xi_1)h_0(\xi_2)$.

The four vertex modes labelled A, B, C, and D are therefore described as:

Vertex A:
$$\phi_{0,0}(\xi_1, \xi_2) = \psi_0^a(\xi_1)\psi_0^a(\xi_2)$$

Vertex B :
$$\phi_{P_1,0}(\xi_1,\xi_2) = \psi_{P_1}^a(\xi_1)\psi_0^a(\xi_2)$$

Vertex C:
$$\phi_{0,P_2}(\xi_1,\xi_2) = \psi_0^a(\xi_1)\psi_{P_2}^a(\xi_2)$$

Vertex D:
$$\phi_{P_1,P_2}(\xi_1,\xi_2) = \psi_{P_1}^a(\xi_1)\psi_{P_2}^a(\xi_2)$$
.

The edge between A and C corresponds to the indices (p = 0, 0 < q < P) and so these edge modes of the expansion $\psi_{pq}(\xi_1, \xi_2)$ are defined as $\psi_{0,q}(\xi_1, \xi_2) = \psi_0^a(\xi_1)\psi_q^a(\xi_2)$ (0 < q < P). The four edges of the quadrilateral expansions are therefore defined as:

Edge AB:
$$\phi_{p,0}(\xi_1, \xi_2) = \psi_p^a(\xi_1)\psi_0^a(\xi_2)$$
 $(0$

Edge CD:
$$\phi_{p,P_2}(\xi_1, \xi_2) = \psi_p^a(\xi_1)\psi_{P_2}^a(\xi_2)$$
 $(0$

Edge AC:
$$\phi_{0,q}(\xi_1, \xi_2) = \psi_0^a(\xi_1)\psi_q^a(\xi_2)$$
 $(0 < q < P_2)$

Edge BD:
$$\phi_{P_1,q}(\xi_1, \xi_2) = \psi_{P_1}^a(\xi_1)\psi_q^a(\xi_2)$$
 $(0 < q < P_2).$

Finally, the interior modes to the quadrilateral expansion are analogously defined as:

Interior modes:
$$\phi_{pq}(\xi_1, \xi_2) = \psi_p^a(\xi_1)\psi_q^a(\xi_2)$$
 $(0 < p, q; p < P_1, q < P_2).$

An explicit listing of the nodal and modal quadrilateral basis is also given in Appendix D.

Three-Dimensional Expansion

A similar construction process to the two-dimensional expansion is possible for the three-dimensional basis, however, we now consider a three-dimensional array spanning the standard hexahedral region (also shown in figure 3.3). For this case

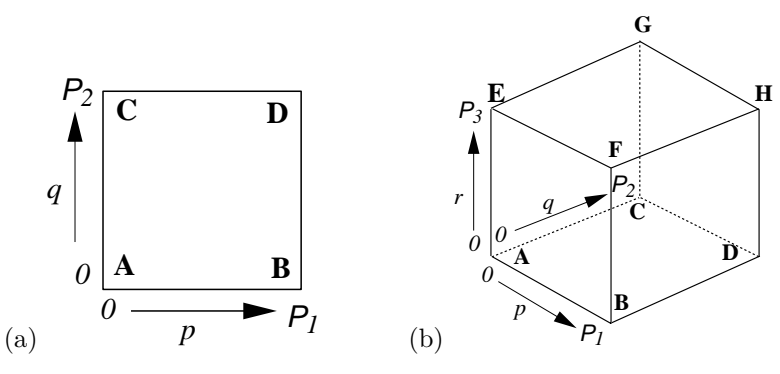


Figure 3.3 Definition of the array indices for the (a) two-dimensional, and (b) three-dimensional tensor expansions.

the modes within the face ABCD correspond to the indices (0 and so these face modes are defined as

$$\phi_{p,q,0}(\xi_1, \xi_2, \xi_3) = \psi_p^a(\xi_1)\psi_q^a(\xi_2)\psi_0^a(\xi_3) \qquad (0$$

To derive the same expansion for the nodal expansion we simply replace $\psi_p^a(\xi)$ with $h_p(\xi)$. For a full listing of the nodal and modal hexahedral bases see Appendix D.

3.1.2 Polynomial Space of Tensor Product Expansions

The expansions $\phi_{pq}(\xi_1, \xi_2)$ and $\phi_{pqr}(\xi_1, \xi_2, \xi_3)$ defined using the tensor product of any of the polynomials $\psi_p^a(\xi), h_p(\xi), L_p(\xi)$ [see equations (3.1), (3.2), and (3.3)] all span the same multi-dimensional polynomial space. This polynomial space is mathematically defined in two dimensions as

$$\phi_{pq}(\xi_1, \xi_2) \subseteq \mathcal{P}_P(\mathcal{Q}^2) = \text{span}\{\xi_1^p \ \xi_2^q\}_{(p,q) \in \Upsilon}$$

 $\Upsilon = \{(p,q) | 0 \le p \le P_1, 0 \le q \le P_2\},$

and in three dimensions as

$$\phi_{pqr}(\xi_1, \xi_2, \xi_3) \subseteq \mathcal{P}_P(\mathcal{Q}^3) = \text{span}\{\xi_1^p \ \xi_2^q \ \xi_3^r\}_{(pqr) \in \Upsilon}$$

$$\Upsilon = \{(p, q, r) | 0 \le p \le P_1, 0 \le q \le P_2, 0 \le r \le P_3\}.$$

In two dimensions, it is normal to consider the polynomial spaces in terms of Pascal's triangle. Figure 3.4 shows, for the expansion $\phi_{pq}(\xi_1,\xi_2)$, the space spanned when $P_1=4$ and $P_2=3$ as well as the hierarchical modes used in this expansion. The definition of the set Υ indicates the range over which the expansion modes $\phi_{pq}(\xi_1,\xi_2),\phi_{pqr}(\xi_1,\xi_2,\xi_3)$ must be assembled if they are to span the complete polynomial basis, (that is, $0 \le p \le P_1, 0 \le q \le P_2, 0 \le r \le P_3$). Therefore, for an expansion to span the complete space up to $\xi_1^{P_1}\xi_2^{P_2}\xi_3^{P_3}$ requires $(P_1+1)(P_2+1)$ modes in two dimensions, and $(P_1+1)(P_2+1)(P_3+1)$ modes in three dimensions.

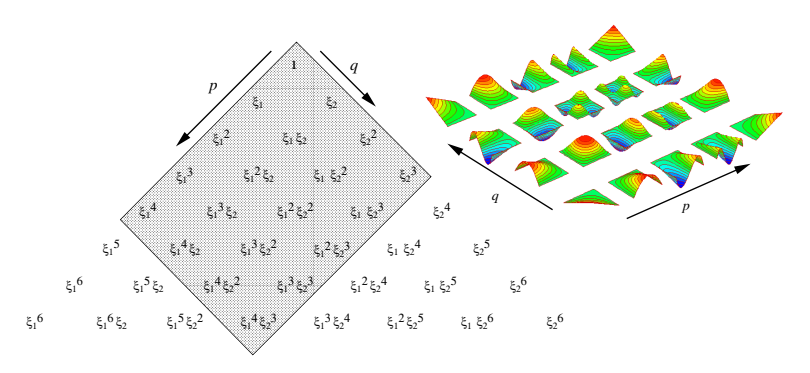


Figure 3.4 Polynomial space in terms of the Pascal's triangle of the full tensor product quadrilateral expansion with $P_1 = 4$ and $P_2 = 3$.

A broad range of modal expansions is possible due to the variety of combinations of edge, face, and interior modes. In the most general case we can describe a modal expansion which has a boundary/interior decomposition with an independent parameter to bound the modes along every edge, two independent parameters to bound the modes within every face, and another three parameters to bound the interior modes. This type of flexibility is desirable as it provides a relatively natural way to vary the expansion order from one elemental domain to another while maintaining C^0 continuity. The adaptivity of the polynomial space may also be introduced using the non-conforming techniques as discussed in chapter 7.

3.1.2.1 Serendipity Expansion

The hierarchical nature of the modal expansion gives rise to a greater flexibility in that it permits the use of a reduced number of expansion modes as compared with those in the full tensor space. One widely used modified expansion is the serendipity expansion which does not include the full tensor product of interior modes. In this expansion we only use the modes necessary to produce a horizontal level of the Pascal's triangle, that is,

$$\mathcal{P}_{P}(\mathcal{Q}^{2}) = \operatorname{span}\{\xi_{1}^{p} \ \xi_{2}^{q}\}_{(pq) \in \Upsilon}$$

$$\Upsilon = \{(p, q) | \ 0 \le p, q \le P; p + q \le P\}.$$

This linear space is the natural space for a p-type expansion in a triangular region. The quadrilateral expansion cannot be reduced exactly to this space although it can come very close. To achieve this we retain all the boundary modes and combine them with the interior modes up to the restriction $p+q \leq P-2$. The Pascal triangle and modal shapes for this expansion when $P_1=P_2=P=4$ are shown in figure 3.5. We observe that the reduced quadrilateral expansion is therefore almost identical to the triangular polynomial space except for the two polynomials $\xi_1^4 \xi_2$ and $\xi_1 \xi_2^4$ which are introduced by the edge modes and cannot be removed because they are required for completeness of the expansion.

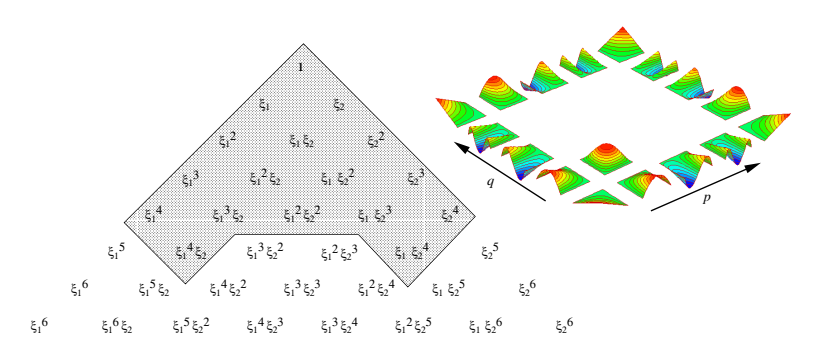


Figure 3.5 Pascal triangle and modal shapes for a P=4 serendipity expansion using all the boundary modes with interior modes supported up to the limit $p+q \leq P-2$ (recall that the interior mode is a polynomial of the form $\xi_1^2 \xi_2^2$).

It is also possible to construct a serendipity nodal expansion which spans a similar space, but this requires modification of the basis definition to permit different order Lagrange polynomials in the interior of the expansion (see[75, 244, 510]] for further discussion). The construction of the Lagrange polynomial is such that a square number of modes are always needed to make a complete expansion and so the polynomial space is slightly richer than the space illustrated in figure 3.5. However, a compatible nodal basis which does match this serendipity space may also be generated using a combination of the nodal and modal expansions [484]. This can destroy some of the inherent efficiency of the full nodal tensor product but permits greater expansion flexibility between domains.

3.2 Generalised Tensor Product Modal Expansions

To extend the tensor product expansion in quadrilateral and hexahedral domains discussed in section 3.2 to simplex regions such as triangular and tetrahedral regions we need to generalise the tensor product expansion concept. In this section we shall introduce modal expansions in subdomains typically associated with unstructured discretisation which in two dimensions typically means the triangular region, and in three dimensions includes the tetrahedral region. A natural extension to the construction of a tetrahedral expansion will also lead to a unified basis which includes pentahedral regions such as prismatic and pyramidic shapes as well as the hexahedral modal expansion discussed previously. We shall refer to the bundle of mixed shapes as hybrid regions.

The use of triangular or tetrahedral spectral/hp element methods in computational fluid dynamics has been relatively limited when compared to quadrilateral and hexahedral spectral/hp element discretisations. An important consideration when using triangular or tetrahedral expansion for time-dependent computations, which typically arise in fluid dynamics, is the numerical efficiency of the algorithm in the context of $cost\ per\ time\ step$. To be competitive, a triangular expansion must be as numerically efficient as the quadrilateral expansion. Since a great deal of the efficiency of the quadrilateral or hexahedral expansion (partic-

ularly at larger polynomial orders) arises from the tensor product construction we would like to use a similar procedure to construct expansions within the triangular or tetrahedral domains.

An orthogonal, generalised tensor product, two-dimensional basis has been proposed by several authors the first of which we believe to be Proriol in 1957 [383]. This basis has also been independently proposed by Karlin & McGregor [257] and Koornwinder [273] (who also constructed orthogonal polynomials for different kinds of domains) as well as more recently by Dubiner [142]. These expansions are also known to be solutions to a singular Sturm-Liouville problem [74, 282, 355, 480, 493]. Dubiner's paper also suggested a modified basis for C^0 continuous expansions and discussed the three-dimensional extension of the orthogonal expansion to a tetrahedral region. The derivation of a C^0 continuous expansion in a tetrahedral region based on Dubiner orthogonal expansion was first presented by Sherwin & Karniadakis [420, 428]. Both the orthogonal and C^0 expansions were presented in a unified approach for hybrid elemental regions by Sherwin in [421]. We shall be adopting the unified approach in this section and we will discuss non-tensorial expansions for simplex regions in section 2.3.4.

An interesting characteristic of these expansions is that the individual expansion modes are not rotationally symmetric in the standard regions. Rotational symmetry has historically been an important consideration when constructing unstructured polynomial expansion bases. The desire for rotational symmetry naturally motivates the use of the rotationally invariant barycentric coordinate systems (see section 3.2.1.3). However, the use of the barycentric coordinate system can destroy much of the numerical efficiency associated with the standard tensor product expansion bases. One way to recover this efficiency is to design a coordinate system based on the mapping of a square to a triangle generating a collapsed coordinate system. The use of a collapsed coordinate system as discussed in 3.2.1 regains some of this efficiency but inherently destroys the rotational symmetry of each mode of the expansion. Nevertheless, these expansions span an identical polynomial space as the traditional unstructured expansions using barycentric coordinates. Therefore, in the absence of any integration error they are equivalent to any other polynomial expansion bases used in a Galerkin approximation. The lack of rotational symmetry does not effect the multi-domain construction of the triangular expansion although for tetrahedral domains it does impose a restriction on orientation of the elemental regions which can be trivially satisfied as will be explained in section 4.2.1. Amongst other applications, these expansion bases have been applied to the incompressible and compressible Navier-Stokes equations (for example see [420, 429, 430, 409, 480, 306) as well as geophysical fluid dynamics problems [492].

Other modal expansions which are available in the literature are included in the book by Szabo and Babuška [442] which documents a modal triangular and tetrahedral expansion based on a barycentric coordinate system (see section 3.2.1.3). These expansions are rotationally non-symmetric and have been applied to structural mechanics problems. Webb and Abouchacra [486] have also developed a hierarchical triangular expansion based on Jacobi polynomials, which

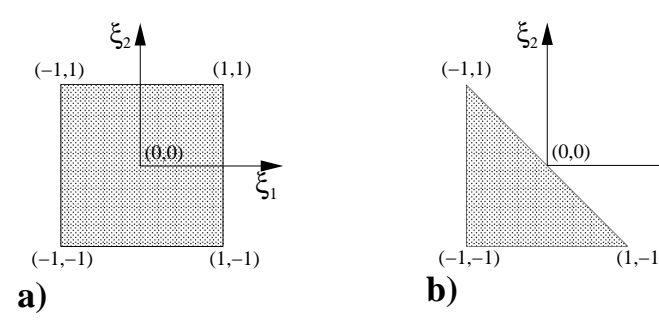


Figure 3.6 Standard regions for the (a) quadrilateral, and (b) triangular expansion in terms of the Cartesian coordinates ξ_1, ξ_2 .

is also rotationally non-symmetric and uses a barycentric coordinate system. Finally, Zambusch [505] has proposed a symmetric hierarchical expansion for triangular and tetrahedral regions based on the barycentric coordinates system but these bases depend on defining a new polynomial space; this basis has also been applied in the area of structural mechanics.

To understand the derivation of the generalised tensor product modal expansion we initially require the definition of a new *collapsed* coordinate system as introduced in section 3.2.1. Using the collapsed coordinate system we can then construct orthogonal polynomial expansions within both simplex regions and the standard quadrilateral and hexahedral regions as discussed in section 3.2.2. Finally, since the orthogonal expansions cannot easily be tessellated into C^0 expansions, we discuss in section 3.2.3 a set of modified expansions which have an interior and boundary decomposition making them suitable for use in a global C^0 continuous expansion.

3.2.1 Coordinate Systems

In the structured expansions discussed in section 3.1 we generated a multidimensional expansion by forming a tensor product of one-dimensional expansions based on a Cartesian coordinate system. The one-dimensional expansion was defined between constant limits and therefore an implicit assumption of the tensor extension was that the coordinates in the two-dimensional region were bounded between constant limits. As illustrated in figure 3.6, within the standard quadrilateral region, the Cartesian coordinates (ξ_1, ξ_2) are bounded by constant limits, that is,

$$Q^2 = \{(\xi_1, \xi_2) | -1 \le \xi_1, \xi_2 \le 1\}.$$

However, as shown in figure 3.6(b), this is not the case in the standard triangular region as the bounds of the Cartesian coordinates (ξ_1, ξ_2) are dependent upon each other, that is,

$$\mathcal{T}^2 = \{(\xi_1, \xi_2) | -1 \le \xi_1, \xi_2; \ \xi_1 + \xi_2 \le 0 \}.$$

Therefore, to develop a suitable tensorial type basis within unstructured regions, such as the triangle, we need to develop a coordinate system where the local coor-

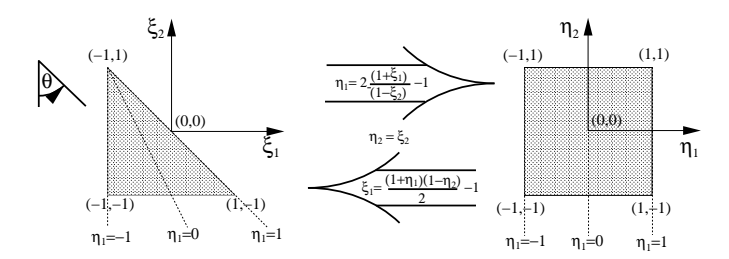


Figure 3.7 Triangle to rectangle transformation.

dinates have independent bounds. The advantage of such a system is that we can then define one-dimensional functions upon which we can construct our multidomain tensorial basis. It also defines an appropriate system upon which we can perform important numerical operations such as integration and differentiation, as discussed in sections 2.4.1 and 2.4.2.

$3.2.1.1 \quad Collapsed \ Two-Dimensional \ Coordinate \ System$

A suitable coordinate system, which describes the triangular region between constant independent limits, is defined by the transformation

$$\eta_1 = 2\frac{(1+\xi_1)}{(1-\xi_2)} - 1
\eta_2 = \xi_2,$$
(3.4)

and has the inverse transformation

$$\xi_1 = \frac{(1+\eta_1)(1-\eta_2)}{2} - 1$$

$$\xi_2 = \eta_2.$$
(3.5)

These new local coordinates (η_1, η_2) define the standard triangular region by

$$\mathcal{T}^2 = \{(\eta_1, \eta_2) | -1 \le \eta_1, \eta_2 \le 1\}.$$

The definition of the triangular region in terms of the coordinate system (η_1, η_2) is identical to the definition of the standard quadrilateral region in terms of the Cartesian coordinates (ξ_1, ξ_2) . This suggests that we can interpret the transformation (3.4) as a mapping from the triangular region to a rectangular one as illustrated in figure 3.7. For this reason, we shall refer to the coordinate system (η_1, η_2) as the collapsed coordinate system. The transformation (3.4) maps the vertical lines in the rectangular domain (lines of constant η_1) onto lines radiating out of the top vertex $(\xi_1 = -1, \xi_2 = 1)$ in the triangular domain. The triangular region is now described by a "ray" coordinate, η_1 , and the standard horizontal coordinate by $(\xi_2 = \eta_2)$. Another consequence of the transformation is that the "ray" coordinate (η_1) is multi-valued at $(\xi_1 = -1, \xi_2 = 1)$. However, we can show that η_1 is bounded at this point by making a change of variables to (ϵ, θ) where

 $\xi_1 = -1 + \epsilon \sin \theta, \xi_2 = 1 - \epsilon \cos \theta$. This change of variables simply expresses the Cartesian coordinates ξ_1, ξ_2 in terms of a cylindrical system (ϵ, θ) centered on the singular points $(\xi_1 = -1, \xi_2 = 1)$, where θ is defined in an anti-clockwise sense from the vertical, as indicated in figure 3.7. Substituting these values into the definition of η_1 given by equation (3.4) we can determine the limiting behavior of the singularity as $\epsilon \to 0$, that is,

$$\eta_1|_{\xi_1=-1,\xi_2=1} = 2\frac{1-1+\epsilon\sin\theta}{1-1+\epsilon\cos\theta} - 1 = 2\tan\theta - 1.$$

Since $0 \le \theta \le \pi/4$ we know that $0 \le \tan \theta \le 1$ and so $-1 \le \eta_1|_{\xi_1 = -1, \xi_2 = 1} \le 1$. Although the introduction of a singularity may seem unfavorable, such singularities naturally occur in cylindrical and spherical coordinate systems.

This type of coordinate system is sometimes referred to as *Duffy coordinates* [143] and is used in boundary element methods to handle the singular integrals.

3.2.1.2 Collapsed Three-Dimensional Coordinate Systems

The interpretation of a triangle to rectangle mapping of the two-dimensional local coordinate system, as illustrated in figure 3.7, is helpful in the construction of a new coordinate system for three-dimensional regions. If we consider the local coordinates (η_1, η_2) as independent axes (although they are not orthogonal) then the coordinate system spans a rectangular region. Therefore, if we start with a hexahedral region and apply the inverse transformation (3.5) we can derive a new local coordinate system in the tetrahedral region \mathcal{T}^3 in three dimensions, where \mathcal{T}^3 is defined as:

$$\mathcal{T}^3 = \{-1 \le \xi_1, \xi_2, \xi_3; \ \xi_1 + \xi_2 + \xi_3 \le -1\}.$$

To reduce the hexahedron to a tetrahedron requires repeated application of the transformation (3.5) as illustrated in figure 3.8. Initially, we consider a hexahedral domain defined in terms of the local coordinate system (η_1, η_2, η_3) where all three coordinates are bounded by constant limits, that is, $(-1 \le \eta_1, \eta_2, \eta_3 \le 1)$. Applying the rectangle-to-triangle transformation (3.5) in the (η_1, η_3) plane we obtain a new ordinate, $\overline{\eta_1}$, such that

$$\frac{\eta_1}{\eta_1} = \frac{(1+\eta_1)(1-\eta_3)}{2} - 1$$
$$\eta_3 = \eta_3.$$

Treating the coordinates $(\overline{\eta_1}, \eta_2, \eta_3)$ as independent, the region which originally spanned a hexahedral domain is mapped to a triangular prism. If we now apply transformation (3.5) in the (η_2, η_3) plane, introducing the ordinates ξ_2, ξ_3 defined as

$$\xi_2 = \frac{(1+\eta_2)(1-\eta_3)}{2} - 1,$$

$$\xi_3 = \eta_3,$$

we see that the coordinates $(-1 \le \overline{\eta_1}, \xi_2, \xi_3 \le 1)$ span a region of a square-based pyramid. The third and final transformation to reach the tetrahedral domain is

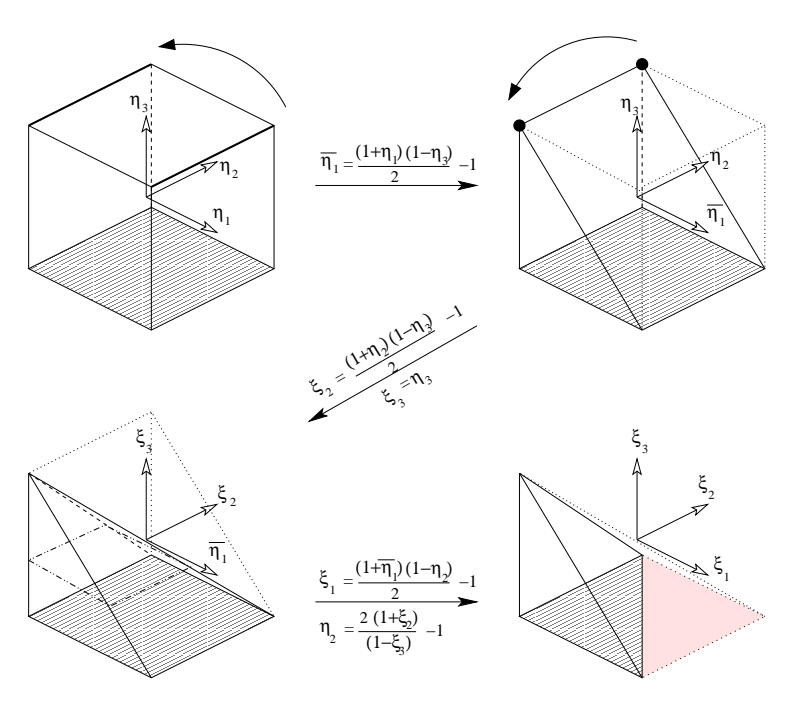


Figure 3.8 Hexahedron to tetrahedron transformation by repeatedly applying the rectangle-to-triangle mapping (3.5).

slightly more subtle, as to reduce the pyramidic region to a tetrahedron we need to apply the mapping in every square cross-section parallel to the $(\overline{\eta_1}, \xi_2)$ plane. This means using the transformation (3.5) in the $(\overline{\eta_1}, \xi_2)$ plane to define the final ordinate (ξ_1) as

$$\xi_1 = \frac{(1 + \overline{\eta_1})(1 - \eta_2)}{2} - 1$$

$$\xi_2 = \xi_2.$$

If we choose to define the coordinate of the tetrahedron region (ξ_1, ξ_2, ξ_3) as the orthogonal Cartesian system, then by determining the hexahedral coordinates (η_1, η_2, η_3) in terms of the orthogonal Cartesian system, we obtain

$$\eta_1 = 2 \frac{(1+\xi_1)}{(-\xi_2 - \xi_3)} - 1, \qquad \eta_2 = 2 \frac{(1+\xi_2)}{(1-\xi_3)} - 1, \qquad \eta_3 = \xi_3, \qquad (3.6)$$

which is a collapsed coordinate system for the tetrahedral domain, and is bounded by constant limits, so the region \mathcal{T}^3 can be defined as

$$\mathcal{T}^3 = \{-1 \le \eta_1, \eta_2, \eta_3 \le -1\}.$$

We also note that when $\xi_3 = -1$ this system reduces to the two-dimensional system defined in (3.4).

Table 3.2 The local collapsed coordinates which have constant bounds within the standard region may be expressed in terms of the Cartesian coordinates ξ_1, ξ_2, ξ_3 . Each region may be defined in terms of the local coordinates as having a lower bound of $-1 \le \xi_1, \xi_2, \xi_3$ and upper bound as indicated in the table. Each region and the planes of constant local coordinates are shown in figure 3.9.

Region	Upper bound	Local col	lapsed coordinate	
Hexahedron	$\xi_1, \xi_2, \xi_3 \le 1$	ξ_1	ξ_2	ξ_3
Prism	$\xi_1 \le 1, \xi_2 + \xi_3 \le 0$	$\overline{\eta_1} = \frac{2(1+\xi_1)}{(1-\xi_3)} - 1$	ξ_2	ξ_3
Pyramid	$\xi_1 + \xi_3, \xi_2 + \xi_3 \le 0$	$\overline{\eta_1} = \frac{2(1+\xi_1)}{(1-\xi_3)} - 1$	$\eta_2 = \frac{2(1+\xi_2)}{(1-\xi_3)} - 1$	$\eta_3 = \xi_3$
Tetrahedron	$\xi_1 + \xi_2 + \xi_3 \le -1$	$\eta_1 = \frac{2(1+\xi_1)}{(-\xi_2-\xi_3)} - 1$	$\eta_2 = \frac{2(1+\xi_2)}{(1-\xi_3)} - 1$	$\eta_3 = \xi_3$

By analogy to this technique, if we had chosen to define the coordinates in either the pyramidic or prismatic region as the orthogonal Cartesian system then evaluating the hexahedral coordinates in terms of these coordinates would generate a collapsed coordinate system for these domains. Table 3.2 shows the local collapsed coordinate systems in all of the three-dimensional regions. A diagrammatic representation of the local collapsed coordinate system is shown in figure 3.9.

3.2.1.3 Barycentric Coordinate Systems

Barycentric coordinate systems otherwise known as area/triangular or volume/tetrahedral coordinates, have historically been used in unstructured domains because of their rotational symmetry. Unlike the quadrilateral or hexahedral regions, in a simplex region such as the triangle and tetrahedron, maintaining symmetry requires an extra (dependent) coordinate which makes the tensor process construction of expansions, as discused in sections 3.1 and 3.2, very difficult if not impossible. Barycentric coordinates will however be useful in defining the rotationally symmetric non-tensorial expansions discussed in this section. We also define the relationship between the barycentric coordinates and volume coordinates and the collapsed coordinate systems discussed in sections 3.2.1.1 and 3.2.1.2

The area coordinate system is illustrated in figure 3.10(a) for the standard triangle. Any point in the triangle is described by three coordinates l_1, l_2 , and l_3 , which can be interpreted as the ratio of the areas A_1, A_2 and A_3 over the total area $A = A_1 + A_2 + A_3$, that is,

$$l_1 = \frac{A_1}{A},$$
 $l_2 = \frac{A_2}{A},$ $l_3 = \frac{A_3}{A}.$

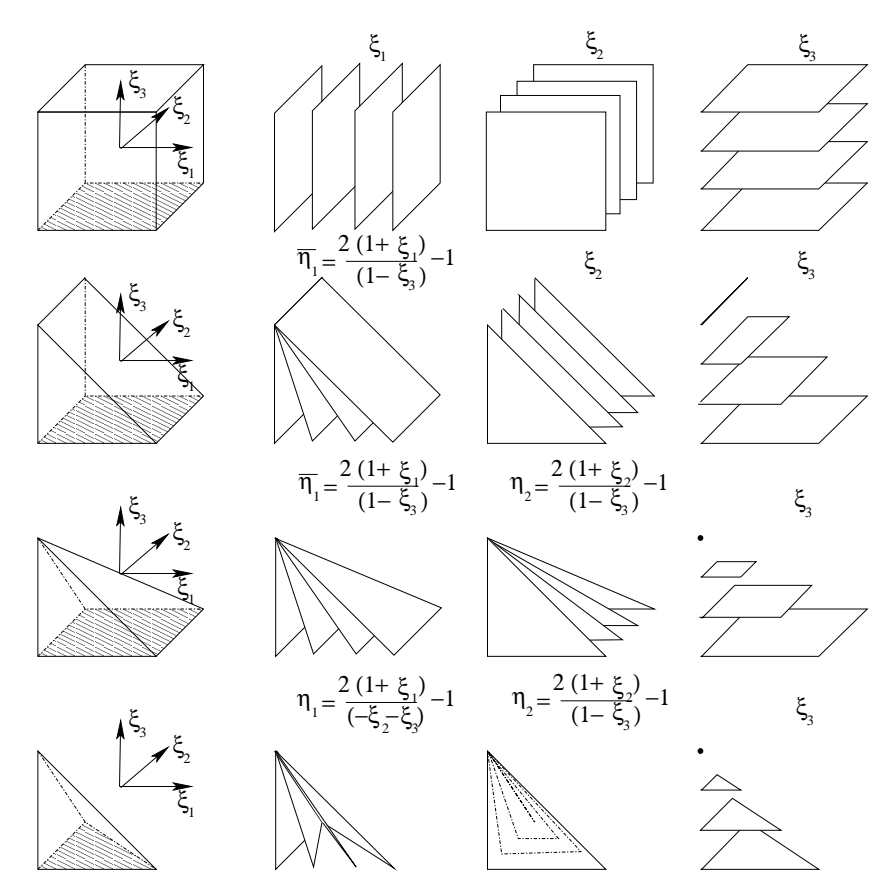


Figure 3.9 Planes of constant value of the local collapsed Cartesian coordinate systems in the hexahedral, prismatic, pyramidic, and tetrahedral domains. In all but the hexahedral domain, the standard Cartesian coordinates ξ_1, ξ_2, ξ_3 describing the region have an upper bound which couples the coordinate system as shown in table 3.2. The local collapsed Cartesian coordinate system $\eta_1, \overline{\eta_1}, \eta_2, \eta_3$ represents a system of non-orthogonal coordinates which are bounded by a constant value within the region.

Therefore l_1 , l_2 , and l_3 have a unit value at the vertices marked 1, 2 and 3 in figure 3.10(a), respectively. By definition these coordinates satisfy the relationship:

$$l_1 + l_2 + l_3 = 1$$
,

and they can be expressed in terms of Cartesian coordinates ξ_1,ξ_2 as:

$$l_1 = \frac{1}{2}(1 - \xi_1) - \frac{1}{2}(1 + \xi_2),$$

$$l_2 = \frac{1}{2}(1 + \xi_1),$$

$$l_3 = \frac{1}{2}(1 + \xi_2).$$

The two-dimensional collapsed coordinate system was defined in sections 3.2.1.1 and 3.2.1.2 as

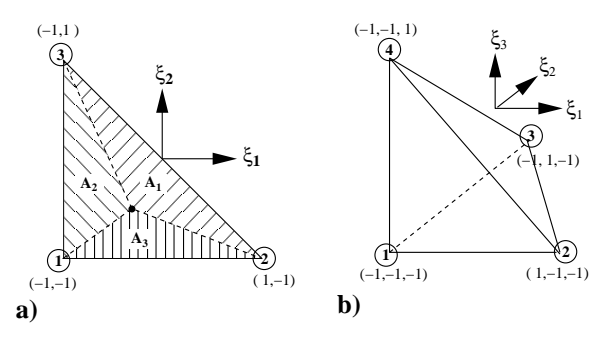


Figure 3.10 (a) The area coordinate system in the standard triangular region. Each coordinate l_1, l_2 , and l_3 can be interpreted as the ratio of areas A_1, A_2 , and A_3 over the total area. (b) The standard tetrahedral region for the definition of volume coordinates.

$$\eta_1 = 2 \frac{(1+\xi_1)}{(1-\xi_2)} - 1$$
 and $\eta_2 = \xi_2$,

which can also be written in terms of the area coordinates as:

$$\eta_1 = \frac{2l_2}{1 - l_3} - 1 = \frac{l_2 - l_1}{1 - l_3}, \qquad \eta_2 = 2l_3 - 1.$$

A similar construction follows for volume coordinates l_1, l_2, l_3, l_4 , which are defined as having a unit value at the vertices marked 1, 2, 3, 4 in figure 3.10(b). In terms of the local Cartesian coordinates the volume coordinate system is defined as:

$$l_1 = \frac{-(1+\xi_1+\xi_2+\xi_3)}{2}, \qquad l_2 = \frac{(1+\xi_1)}{2},$$
$$l_3 = \frac{(1+\xi_2)}{2}, \qquad l_4 = \frac{(1+\xi_3)}{2}.$$

Finally, the three-dimensional collapsed coordinate system for the tetrahedron can be defined in terms of the volume coordinates as:

$$\eta_1 = \frac{2l_2}{(1 - l_3 - l_4)} = \frac{l_2 - l_1}{(1 - l_3 - l_4)},$$

$$\eta_2 = \frac{2l_3}{(1 - l_4)} - 1, \qquad \eta_3 = 2l_4 - 1.$$

3.2.2 Orthogonal Expansions

We have previously seen in chapter 2, section 2.3.2.1 that there are many considerations which motivate a *good* expansion basis. Typically, we are interested in developing a computationally efficient expansion which demonstrates attractive numerical properties such as matrix conditioning or, in the case of convection problems, appropriate explicit time step restrictions (see chapter 6). A reasonable starting point in developing a modal multi-dimensional expansion is to construct

a set of polynomial expansions which are orthogonal in the Legendre inner product (or indeed any desired inner product) over each desired subdomain shape.

In the following section we will discuss a set of orthogonal polynomials in hybrid regions that have a tensor product form [383, 257, 273, 142]. These orthogonal expansions have also been shown to be solutions to singular Sturm-Liouville problems. The first derivation of the Sturm-Liouville problem in a triangle was by Krall and Sheffer in 1967 [282]. Subsequently, this result has also been reported by Owens [355], Wingate & Taylor [493], Warburton [480], and Braess & Schwab [74]. The last three publications also deal with tetrahedral domains.

We saw in section 3.1 how the structured expansions for a quadrilateral and hexahedral domain can be constructed using a product of two one-dimensional tensors. When we use the collapsed coordinate systems introduced in section 3.2.1, we find that a similar extension process is possible for all the unstructured domains using a warped [142] or generalised product involving tensors of two and three dimensions. Unlike the structured two-dimensional tensor product form, where the expansion is constructed from the same one-dimensional basis, the L^2 orthogonal expansion has the form

$$\phi_{pq}(\xi_1, \xi_2) = L_p(\xi_1) L_q(\xi_2),$$

where a more general product is used combining a one-dimensional tensor $\widetilde{\psi}_p^a(z)$ with a two-dimensional tensor of the form $\widetilde{\psi}_{pq}^b(z)$ that is,

$$\phi_{pq}(\xi_1, \xi_2) = \widetilde{\psi}_p^a(\eta_1) \widetilde{\psi}_{pq}^b(\eta_2).$$

Figure 3.11 illustrates the construction of the two-dimensional expansion modes using this more general form. To generate each mode the function $\widetilde{\psi}_p^a(\eta_1)$ is combined with $\widetilde{\psi}_{pq}^b(\eta_2)$. However, unlike the quadrilateral expansion, $\widetilde{\psi}_{pq}^b(\eta_2)$ now has a different form for every value of p of the principal function $\widetilde{\psi}_p^a(\eta_1)$.

This form still maintains the numerical efficiencies which can be achieved from the one-dimensional nature of the expansion using the sum-factorisation process discussed in section 4.1.6. We shall refer to the functions $\tilde{\psi}_p^a(z)$ and $\tilde{\psi}_{pq}^b(z)$ as well as a third function $\tilde{\psi}_{pqr}^c(z)$ as the orthogonal principal functions [421], where $\tilde{\psi}_{pqr}^c(z)$ is required for the three-dimensional expansions. In section 3.2.3 we shall introduce a modified version of the principal functions which are more suitable for multiple domain expansions.

3.2.2.1 Orthogonal Expansions in Hybrid Domains Based on One Dimensional Principal Functions

Recalling that the function $P_p^{\alpha,\beta}(z)$ denotes the pth-order Jacobi polynomial introduced in section 2.3.3.1 (see also Appendix A) the principal functions, $\widetilde{\psi}_p^a(z)$, $\widetilde{\psi}_{pqr}^b(z)$, $\widetilde{\psi}_{pqr}^c(z)$, for orthogonal expansions in hybrid domains are:

$$\widetilde{\psi}^a_p(z) = P^{0,0}_p(z), \qquad \quad \widetilde{\psi}^b_{pq}(z) = \left(\frac{1-z}{2}\right)^p P^{2p+1,0}_q(z),$$

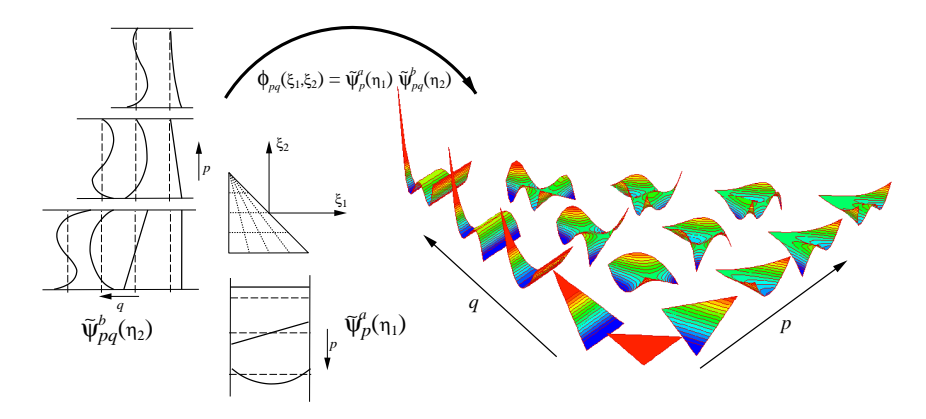


Figure 3.11 Construction of two-dimensional expansion modes $\phi_{pq}(\xi_1, \xi_2)$ within a triangular region using the product of a one-dimensional tensor $\widetilde{\psi}_p^a(\eta_1(\xi_1, \xi_2))$ and a two-dimensional tensor $\widetilde{\psi}_{pq}^b(\eta_2(\xi_2))$.

$$\widetilde{\psi}^c_{pqr}(z) = \left(\frac{1-z}{2}\right)^{p+q} P_k^{2p+2q+2,0}(z).$$

The two-dimensional expansions in terms of the principal functions are defined as:

Quadrilateral expansion:
$$\phi_{pq}(\xi_1, \xi_2) = \widetilde{\psi}_p^a(\xi_1) \widetilde{\psi}_q^a(\xi_2),$$

Triangular expansion: $\phi_{pq}(\xi_1, \xi_2) = \widetilde{\psi}_p^a(\eta_1)\widetilde{\psi}_{pq}^b(\eta_2),$

where

$$\eta_1 = \frac{2(1+\xi_1)}{(1-\xi_2)} - 1, \quad \eta_2 = \xi_2,$$

are the two-dimensional collapsed coordinates illustrated in figure 3.7. The shape of all the triangular modes for a fourth-order polynomial expansion are shown in figure 3.11.

The three-dimensional expansions are defined in terms of the principal functions as:

Hexahedral expansion: $\phi_{pqr}(\xi_1, \xi_2, \xi_3) = \widetilde{\psi}_p^a(\xi_1) \ \widetilde{\psi}_q^a(\xi_2) \ \widetilde{\psi}_r^a(\xi_3),$

Prismatic expansion: $\phi_{par}(\xi_1, \xi_2, \xi_3) = \widetilde{\psi}_n^a(\overline{\eta_1}) \ \widetilde{\psi}_a^a(\xi_2) \ \widetilde{\psi}_{pr}^b(\xi_3),$

Pyramidic expansion: $\phi_{pqr}(\xi_1, \xi_2, \xi_3) = \widetilde{\psi}^a_p(\overline{\eta_1}) \ \widetilde{\psi}^a_q(\eta_2) \ \widetilde{\psi}^c_{pqr}(\eta_3),$

Tetrahedral expansion: $\phi_{pqr}(\xi_1, \xi_2, \xi_3) = \widetilde{\psi}_p^a(\eta_1) \ \widetilde{\psi}_{pq}^b(\eta_2) \ \widetilde{\psi}_{pqr}^c(\eta_3),$

where

$$\eta_1 = \frac{2(1+\xi_1)}{(-\xi_2-\xi_3)} - 1, \quad \overline{\eta_1} = \frac{2(1+\xi_1)}{(1-\xi_3)} - 1, \quad \eta_2 = \frac{2(1+\xi_2)}{(1-\xi_3)} - 1, \quad \eta_3 = \xi_3,$$

are the three-dimensional collapsed coordinates illustrated in figure 3.9.

Formulation

note: Definition of orthogonal modal expansions in 2D standard hybrid regions.

Formulation

note: Definition of orthogonal modal expansions in 3D standard hybrid regions.

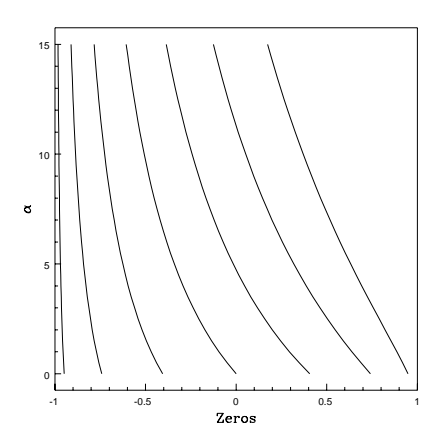


Figure 3.12 Location of the zeros of the Jacobi polynomial $P_i^{\alpha,0}(z)$ $(i \leq 7)$ in the interval [-1,1] for integer values of α , $0 \leq \alpha \leq 15$. For increasing α we see there is a declustering of the zeros away from the point z=1.

These expansions are all polynomials in terms of both their local collapsed coordinates and the Cartesian coordinates. The structured expansions in the quadrilateral and hexahedral domains are simply standard tensor products of Legendre polynomials in terms of Cartesian coordinates since $P_p^{0,0}(z) = L_p(z)$. The development of unstructured expansions using the local collapsed coordinate systems is linked to the use of the more general functions $\widetilde{\psi}_{pq}^b(z)$ and $\widetilde{\psi}_{pqr}^c(z)$. These functions both contain factors of the form $\left(\frac{1-z}{2}\right)^n$ which are necessary to keep the expansions as polynomials in terms of the Cartesian coordinates (ξ_1,ξ_2,ξ_3) . For example, the coordinate η_1 in the triangular expansion necessitates the use of the function $\widetilde{\psi}_{pq}^b(\eta_2)$ (where $\eta_2=\xi_2$) which introduces a factor of $\left(\frac{1-\xi_2}{2}\right)^p$. The product of this factor with $\widetilde{\psi}_p^a(\eta_1)$ is a polynomial function in ξ_1 and ξ_2 . A similar argument supports the introduction of the local coordinate η_2 in the prismatic expansions. The local coordinate system in the pyramidic domains introduces a second collapsed coordinate $\overline{\eta_1}$ which requires the introduction of the principal function $\widetilde{\psi}_{pqr}^c(\eta_3)$. The expansion in the tetrahedral regions uses the additional collapsed coordinate $\eta_1=\frac{2(1+\xi_1)}{(-\xi_2-\xi_3)}-1$ (recall that this is the same as the two-dimensional definition when $\xi_3=-1$). Noting that $-\xi_2-\xi_3$ can be expressed in terms of η_2 and η_3 as

$$-\xi_2 - \xi_3 = \frac{1}{2}(1 - \eta_2)(1 - \eta_3),$$

we see that the polynomial $\widetilde{\psi}_p^a(\eta_1)$ becomes a polynomial in ξ_1, ξ_2 , and ξ_3 if we multiply it by the factor $(1-\eta_2)^p(1-\eta_3)^p$. This factor is incorporated in the principal functions $\widetilde{\psi}_{pq}^b(\eta_2)$ and $\widetilde{\psi}_{pqr}^c(\eta_3)$.

The principal functions $\widetilde{\psi}_{pq}^b(\eta_2)$ and $\widetilde{\psi}_{pqr}^c(\eta_3)$ also contain a Jacobi polynomial of the form $P_i^{\alpha,0}(z)$. As can be seen from figure 3.12, for increasing values of α this polynomial has zeros which are declustered away from the point z=+1. As noted in [484] this declustering is important in maintaining the linear independence of the expansion leading to well-conditioned numerical systems.

3.2.2.2 Demonstration of Orthogonality

To gain an insight into the use of the Jacobi polynomial $P^{\alpha,0}(z)$ in defining the principal functions $\widetilde{\psi}_{pq}^b(z)$ and $\widetilde{\psi}_{pqr}^c(z)$ we shall demonstrate the orthogonality of the triangular and tetrahedral expansion in the Legendre inner product, that is,

$$\int_{\Omega_{st}} \phi_{pqr}(\xi_1, \xi_2, \xi_3) \phi_{ijk}(\xi_1, \xi_2, \xi_3) \ d\xi_1 d\xi_2 d\xi_3 \tag{3.7}$$

where Ω_{st} denotes the appropriate standard region, i.e. triangle (\mathcal{T}^2) or tetrahedron (\mathcal{T}^3).

Orthogonality of the Triangular Expansion

Considering the triangular expansion in the standard region

$$\phi_{pq}(\xi_1, \xi_2) = \widetilde{\psi}_p^a(\eta_1) \widetilde{\psi}_{pq}^b(\eta_2),$$

equation (3.7) can be written in terms of the local coordinate system η_1, η_2 as:

$$\int_{-1}^{1} \int_{-1}^{-\xi_2} \phi_{pq} \phi_{ij} d\xi_1 \ d\xi_2 = \int_{-1}^{1} \int_{-1}^{1} \widetilde{\psi}_p^a(\eta_1) \widetilde{\psi}_{pq}^b(\eta_2) \widetilde{\psi}_i^a(\eta_1) \widetilde{\psi}_{ij}^b(\eta_2) J d\eta_1 d\eta_2,$$

where

$$J = \frac{\partial(\xi_1, \xi_2)}{\partial(\eta_1, \eta_2)} = \frac{1 - \eta_2}{2}.$$

Since the expansion is a product of polynomials in terms of the local coordinates η_1, η_2 and because the Jacobian is only a function of η_2 , the inner product can be expressed in terms of two one-dimensional integrals:

$$\int_{-1}^{1} \widetilde{\psi}_{p}^{a} \widetilde{\psi}_{i}^{a} d\eta_{1} \int_{-1}^{1} \widetilde{\psi}_{pq}^{b} \widetilde{\psi}_{ij}^{b} \left(\frac{1-\eta_{2}}{2}\right) d\eta_{2}. \tag{3.8}$$

Recalling the definitions of the principal functions,

$$\widetilde{\psi}_{p}^{a}(\eta_{1}) = P_{p}^{0,0}(\eta_{1}), \quad \widetilde{\psi}_{pq}^{b}(\eta_{2}) = \left(\frac{1-\eta_{2}}{2}\right)^{p} P_{q}^{2p+1,0}(\eta_{2})$$

we see that the first integral in equation (3.8) contains the standard Legendre polynomials $(P_p^{0,0}(z) = L_p(z))$ which are orthogonal in the interval [-1,1]. Accordingly, this integral is zero unless p=i when it is equal to $\frac{2}{2p+1}$. The second integral can be written in full as

$$\int_{-1}^{1} \left(\frac{1-\eta_2}{2}\right)^p P_q^{2p+1,0}(\eta_2) \cdot \left(\frac{1-\eta_2}{2}\right)^i P_j^{2i+1,0}(\eta_2) \left(\frac{1-\eta_2}{2}\right) d\eta_2.$$

The Jacobi polynomial $P_r^{2p+1,0}(\eta_2)$ is orthogonal in this interval with respect to the weight function $\left(\frac{1-\eta_2}{2}\right)^{(2p+1)}$ [see equation (A.7) in Appendix A], and therefore if p=i the integral is zero except when q=j. However, if $p\neq i$ the first integral in equation (3.8) is necessarily zero and so the expansion $\phi_{pq}(\xi_1,\xi_2)$ is orthogonal to $\phi_{ij}(\xi_1,\xi_2)$ in the standard region \mathcal{T}^2 .

Orthogonality of the Tetrahedral Expansion

Orthogonality of the tetrahedral expansions follows from a similar construction to that previously shown for the triangular expansions. Expressing the basis ϕ_{pqr} in terms of its product form of the principal functions, the Legendre inner product (3.7) can be written as:

$$\int_{-1}^{1} \int_{-1}^{-\xi_{3}} \int_{-1}^{-1-\xi_{2}-\xi_{3}} \phi_{pqr} \phi_{ijk} \ d\xi_{1} \ d\xi_{2} \ d\xi_{3} = \int_{-1}^{1} \int_{-1}^{1} \int_{-1}^{1} \int_{-1}^{1} \widetilde{\psi}_{p}^{a} \widetilde{\psi}_{pq}^{b} \widetilde{\psi}_{pqr}^{c} \ \widetilde{\psi}_{i}^{a} \widetilde{\psi}_{ij}^{b} \widetilde{\psi}_{ijk}^{c} J \ d\eta_{1} d\eta_{2} d\eta_{3},$$

where η_1, η_2, η_3 are the three-dimensional collapsed coordinates and

$$J = \frac{\partial(\xi_1, \xi_2, \xi_3)}{\partial(\eta_1, \eta_2, \eta_3)} = \left(\frac{1 - \eta_2}{2}\right) \left(\frac{1 - \eta_3}{2}\right)^2.$$

Since the basis is a product of the three principal functions and the Jacobian J can also be expressed as a product of two functions in terms of the local coordinates, the integral can be written as a product of the three one-dimensional integrals of the form:

$$\int_{-1}^{1} \widetilde{\psi}_{pq}^{a} \widetilde{\psi}_{i}^{a} d\xi_{1} \mapsto \int_{-1}^{1} P_{p}^{0,0}(\eta_{1}) P_{i}^{0,0}(\eta_{1}) d\eta_{1} \qquad (3.9a)$$

$$\int_{-1}^{1} \widetilde{\psi}_{pq}^{b} \widetilde{\psi}_{ij}^{b} \left(\frac{1-\eta_{2}}{2}\right) d\xi_{2} \mapsto \int_{-1}^{1} P_{p}^{2p+1,0}(\eta_{2}) P_{i}^{2i+1,0}(\eta_{2}) \left(\frac{1-\eta_{2}}{2}\right)^{p+i+1} d\eta_{2} \qquad (3.9b)$$

$$\int_{-1}^{1} \widetilde{\psi}_{pqr}^{c} \widetilde{\psi}_{ijk}^{c} \left(\frac{1-\eta_{3}}{2}\right)^{2} d\xi_{3} \mapsto \int_{-1}^{1} P_{r}^{2p+2q+2,0}(\eta_{3}) \cdot P_{k}^{2i+2j+2,0}(\eta_{3}) \left(\frac{1-\eta_{3}}{2}\right)^{(p+q)+(i+j)+2} d\eta_{3}. \qquad (3.9c)$$

As discussed in the previous section, equation (3.9a) is the inner product of the Legendre polynomial which is zero if $p \neq i$. The integral in equation (3.9b) is zero if $q \neq j$ when p = i since when p = i this integral becomes the orthogonality relation for the Jacobi polynomials $P_p^{2p+1,0}(\eta_1)$ as given in Appendix A. Finally,

integral (3.9c) is zero if $r \neq k$ when p = i and q = j because the integral becomes the orthogonality relation for the Jacobi polynomial $P_r^{2p+2q+2,0}(\eta_3)$.

We can appreciate that, unlike the structured hexahedral expansion where each one-dimensional integral gives an independent orthogonal relation, the tetrahedral expansion requires the orthogonality of the first integral to support the second, and the orthogonality of the first and second integral to support that of the third integral. This has implications for the ordering of the modes when dealing with the modified expansion in section 3.2.3.

3.2.2.3 Singular Sturm-Liouville Equations of the Orthogonal Expansions

We have previously noted that the Jacobi polynomials are the solution to a singular Sturm-Liouville problem. This is significant, since as discussed in section 2.5.2, the convergence of a numerical approximation based on expansion bases which satisfy singular Sturm-Liouville problems demonstrates spectral convergence if the approximated function is sufficiently smooth. The natural extension of this one-dimensional result to a quadrilateral region is the tensor product expansion

$$\phi_{pq}(\xi_1, \xi_2) = P_p^{0,0}(\xi_1) P_q^{0,0}(\xi_2)$$

which satisfies the singular Sturm-Liouville equation

$$\frac{\partial}{\partial \xi_1} \left[(1 - \xi_1^2) \frac{\partial \phi_{pq}}{\partial \xi_1} \right] + \frac{\partial}{\partial \xi_2} \left[(1 - \xi_2^2) \frac{\partial \phi_{pq}}{\partial \xi_2} \right] + \lambda_{pq} \ \phi_{pq} = 0 \tag{3.10}$$

where $\lambda_{pq} = p(p+1) + q(q+1)$. This equation is invariant under all rotations and reflections in the square. A defining feature of this equation, as discussed in [493], is that along each edge ($\xi_1 = \pm 1, \xi_2 = \pm 1$) where the derivative is tangential, there is a quadratic coefficient which goes to zero on all sides not tangential to the direction of differentiation. These features are important to make the differential operator self-adjoint.

The extension from a one-dimensional segment to a two-dimensional quadrilateral region is relatively intuitive. However, not quite as intuitive is the singular Sturm-Liouville for the triangular region as investigated in [282, 355, 480, 493]. We start our discussion by noting that the orthogonal expansion in a triangle

$$\phi_{pq}(\xi_1, \xi_2) = P_p^{0,0}(\eta_1) \left(\frac{1 - \eta_2}{2}\right)^p P_q^{2p+1,0}(\eta_2)$$
(3.11)

satisfies the singular Sturm-Liouville equation

$$\frac{2}{(1-\eta_2)} \left\{ \frac{\partial}{\partial \eta_1} \left[(1-\eta_1^2) \frac{\partial \phi_{pq}}{\partial \eta_1} \right] + \frac{\partial}{\partial \eta_2} \left[(1-\eta_2^2) \frac{(1-\eta_2)}{2} \frac{\partial \phi_{pq}}{\partial \eta_2} \right] \right\} + \lambda_{pq} \ \phi_{pq} = 0, \quad (3.12)$$

where

$$\lambda_{pq} = (p+q)(p+q+2)$$
 and $\eta_1 = \frac{2(1+\xi_1)}{(1-\xi_2)} - 1, \ \eta_2 = \xi_2.$

We see from equation (3.12) that the form of the triangular singular Sturm-Liouville equation, similar to equation (3.10), contains quadratic or higher coefficients which are zero on the boundary of the region defined along $\eta_1 = \pm 1$, $\eta_2 = \pm 1$.

To demonstrate that the orthogonal basis (3.11) satisfies equation (3.12) we follow the formulation used by Warburton [480] and initially consider the second differential term in equation (3.12) which on substitution of expansion (3.11) can be written as

$$\begin{split} \frac{2}{(1-\eta_2)} \frac{\partial}{\partial \eta_2} \left[(1-\eta_2^2) \frac{(1-\eta_2)}{2} \frac{\partial \phi_{pq}}{\partial \eta_2} \right] = \\ \frac{2P_p^{0,0}}{(1-\eta_2)} \frac{\partial}{\partial \eta_2} \left[-p(1+\eta_2) \left(\frac{1-\eta_2}{2} \right)^{p+1} P_q^{2p+1,0} + (1-\eta_2^2) \left(\frac{1-\eta_2}{2} \right)^{p+1} \frac{\partial P_q^{2p+1,0}}{\partial \eta_2} \right] = \\ \left(\frac{1-\eta_2}{2} \right)^p P_p^{0,0} \left[(1-\eta_2^2) \frac{\partial^2 P_q^{2p+1,0}}{\partial \eta_2^2} + (-(2p+1) - (2p+3)\eta_2) \frac{\partial P_q^{2p+1,0}}{\partial \eta_2} - p(p+2) P_q^{2p+1,0} - \left(\frac{2}{1-\eta_2} \right) p(p+1) P_q^{2p+1,0} \right]. (3.13) \end{split}$$

Now if we apply relationship (A.2) expressed in terms of the Jacobi polynomial $P_p^{0,0}(\eta)$, then we observe that the first differention term in equation (3.12) can be written

$$\frac{2}{(1-b)}\frac{\partial}{\partial \eta_1} \left[(1-\eta_1^2) \frac{\partial \phi_{pq}}{\partial \eta_1} \right] = \left(\frac{1-\eta_2}{2} \right)^{p-1} P_q^{2p+1,0}(\eta_2) \frac{\partial}{\partial \eta_1} \left[(1-\eta_1^2) \frac{\partial P_p^{0,0}}{\partial \eta_1} \right] \\
= -\left(\frac{2}{1-\eta_2} \right) p(p+1) \phi_{pq}. \tag{3.14}$$

We now note that the last term in equation (3.13) exactly cancels (3.14). Finally we apply equation (A.1) in terms of Jacobi polynomial $P_q^{2p+1,0}(\eta_2)$, to re-express the two differential terms in equation (3.13) as

$$(1-\eta_2^2)\frac{\partial^2 P_q^{2p+1,0}}{\partial \eta_2^2} + \left(-(2p+1) - (2p+3)\eta_2\right)\frac{\partial P_q^{2p+1,0}}{\partial \eta_2} = -p(p+2p+2)P_q^{2p+1,0}.$$

This term combined with $p(p+2)P_q^{2p+1,0}$ exactly balances the non-differential term in equation (3.12) thereby demonstrating that the basis (3.11) is a solution to the Sturm-Liouville equation (3.12).

The eigenvalues of both the quadrilateral and triangular singular Sturm-Liouville equation do not uniquely correspond to a single eigenfunction as was the case for the one-dimensional equation. In the multi-dimensional problem a single eigenvalue $\lambda=\mathcal{C}$ corresponds to a family of eigenfunctions. As noted by

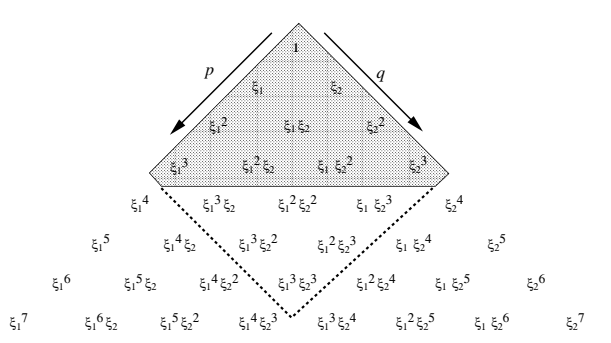


Figure 3.13 Polynomial space in terms of a Pascal's triangle for the triangular expansion (shaded region) and quadrilateral expansion (shaded region plus values within dotted line) when $P_1 = P_2 = 3$.

Wingate & Taylor [493] the commonly used triangular polynomial space (see section 3.2.2.4) corresponds to a union of these eigenspaces for all eigenvalues less than a constant. This can be appreciated from the eigenvalue definition since for $\lambda_{pq} = (p+q)(p+q+2)$ to be a constant requires (p+q) to be constant. A fixed value of (p+q) = P corresponds to all eigenfunctions of polynomial order P. Finally we note that the singular Sturm Liouville equation (3.12) can be written in terms of Cartesian coordinates as

$$\begin{split} &\frac{\partial}{\partial \xi_1} \left((1+\xi_1) \left[(1-\xi_1) \frac{\partial \phi}{\partial \xi_1} - (1+\xi_2) \frac{\partial \phi}{\partial \xi_2} \right] \right) \\ &+ &\frac{\partial}{\partial \xi_2} \left((1+\xi_2) \left[(1-\xi_2) \frac{\partial \phi}{\partial \xi_2} - (1+\xi_1) \frac{\partial \phi}{\partial \xi_1} \right] \right) + \lambda \phi = 0. \end{split}$$

Similar singular Sturm-Liouville equations can also be derived for the hexahedral, prismatic and tetrahedral expansion as discussed in [480, 493]. However, the pyramidic expansion is not encompassed in the same analysis.

3.2.2.4 Polynomial Space of Bases and Assembly of Expansions

The polynomial spaces, in Cartesian coordinates, for the two-dimensional expansions are:

$$\mathcal{P} = \operatorname{Span}\{\xi_1^p \ \xi_2^q \ \}_{(pq) \in \Upsilon} \tag{3.15}$$

where Υ for each domain is

- Quadrilateral $\Upsilon = \{(pq)|0 \le p,q;\ q \le P_1;\ q \le P_2\}$
- Triangular $\Upsilon = \{(pq) | 0 \le p, q; \ q \le P_1; \ p+q \le P_2; \ P_1 \le P_2 \}.$

The polynomial spaces for the case when $P_1 = P_2 = 3$ for both the quadrilateral and triangular expansions are shown in figure 3.13.

The polynomial spaces, in Cartesian coordinates, for the three-dimensional expansions are:

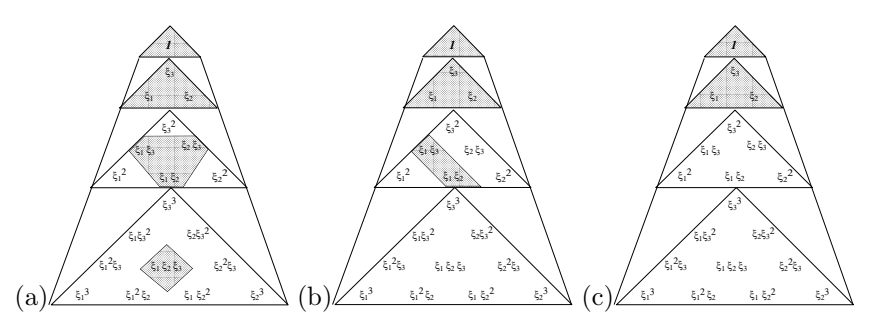


Figure 3.14 Pascal's diagram demonstrating the polynomial space of the orthogonal expansion when $P_1 = P_2 = P_3 = 1$. (a) Hexahedral expansion, (b) Prismatic expansion, (c) Pyramidic and Tetrahedral expansion.

$$\mathcal{P} = \operatorname{Span}\{\xi_1^p \ \xi_2^q \ \xi_3^r\}_{(par) \in \Upsilon} \tag{3.16}$$

where Υ for each domain is

• Hexahedron:

$$\Upsilon = \{(pqr) | 0 \le p, q, r; p \le P_1; q \le P_2; r \le P_3\}$$

• Prism:

$$\Upsilon = \{ (pqr) | 0 \le p, q, r; \ p \le P_1; \ q \le P_2; \ p + r \le P_3; \ P_1 \le P_3 \}$$

• Pyramid: (3.17)
$$\Upsilon = \{(pqr) | 0 \le p, q, r; \ p \le P_1; \ q \le P_2; \ p+q+r \le P_3; \ P_1, P_2 \le P_3\}$$

• Tetrahedron:

$$\Upsilon = \{ (pqr) | 0 \le p, q, r; \ p \le P_1; \ p + q \le P_2; \\ p + q + r \le P_3; \ P_1 \le P_2 \le P_3 \}.$$

The range of p, q, and r indicate how the expansions should be assembled to generate an expansion with a complete polynomial space. As illustrated in figure 3.14, when $P_1 = P_2 = P_3$ the tetrahedral and pyramidic expansions span the same space and are in a subspace of the prismatic expansion, which is in turn a subspace of the hexahedral expansion.

3.2.3 Modified C^0 Expansions

Although the orthogonality of the expansions in section 3.2.2 is attractive these expansions are not normally the most suitable expansions for a general spectral/hp element discretisation. For example, if we are using a standard Galerkin formulation then the global expansion is normally required to have C^0 continuity between elemental domains. The work by Dubiner [142] first discussed the modification of the triangular orthogonal expansions of section 3.2.2 into a semi-orthogonal expansion suitable to generate C^0 continuous global expansions. The modified semi-orthogonal expansion was subsequently extended to three-dimensions by Sherwin & Karniadakis [428] and Sherwin [421]. We note, however, that the

orthogonal bases can still be useful when considering discontinuous Galerkin formulation. Although it is theoretically possible to assemble the orthogonal expansion into multiple regions and enforce a degree of continuity between elemental regions, such an assembly will in practice destroy the orthogonality of the global expansion.

Similar to the discussion in section 2.3.2.1, we can develop an expansion amenable to enforcing C^0 continuity globally by decomposing the orthogonal expansions into an interior and boundary contribution. We will require that the interior modes (or bubble functions) are zero on the boundary of the local elemental domain. The completeness of the expansion is then ensured by adding boundary modes which consist of vertex, edge, and face contributions. The vertex modes have unit value at one vertex and decay to zero at all other vertices; edge modes have local support along one edge and are zero on all other edges and vertices; face modes have local support on one face and are zero on all other faces, edges, and vertices. Using this decomposition, C^0 continuity between elements can be enforced by matching similar shaped boundary modes, see [430].

3.2.3.1 Modified Principal Functions

Analogous to orthogonal expansion we define three principal functions denoted by $\psi_{ij}^a(z), \psi_{ij}^b(z)$ and $\psi_{ijk}^c(z)$ $(0 \le i \le I, \ 0 \le j \le J, \ 0 \le k \le K)$:

$$\psi_i^a(z) = \begin{cases} \left(\frac{1-z}{2}\right) & i = 0\\ \left(\frac{1-z}{2}\right) \left(\frac{1+z}{2}\right) P_{i-1}^{1,1}(z) \ 1 \le i < I \ , \end{cases}$$

$$\left(\frac{1+z}{2}\right) \qquad i = I$$
(3.18)

$$\psi_{ij}^{b}(z) = \begin{cases} \psi_{j}^{a}(z) & i = I \\ \left(\frac{1-z}{2}\right)^{i+1} & 1 \le i < I, \ j = 0 \\ \left(\frac{1-z}{2}\right)^{i+1} \left(\frac{1+z}{2}\right) P_{j-1}^{2i+1,1}(z) \ 1 \le i < I, \ 1 \le j < J \\ \psi_{j}^{a}(z) & i = I, \quad 0 \le j \le J \end{cases}$$

$$(3.19)$$

$$\psi_{ijk}^{c}(z) = \begin{cases} \psi_{jk}^{b}(z) & i = 0, & 0 \le j \le J, \ 0 \le k \le K \\ \psi_{ik}^{b}(z) & 0 \le i \le I, \ j = 0, & 0 \le k \le K \\ \left(\frac{1-z}{2}\right)^{i+j+1} & 1 \le i < I, \ 1 \le j < J, \ k = 0 \\ \left(\frac{1-z}{2}\right)^{i+j+1} \left(\frac{1+z}{2}\right) P_{k-1}^{2i+2j+1,1}(z) \ 1 \le i < I, \ 1 \le j < J \ 1 \le k < K \end{cases}$$

$$\psi_{ik}^{b}(z) & 0 \le i \le I, \ j = J, & 0 \le k \le K \\ \psi_{jk}^{b}(z) & i = I, & 0 \le j \le J, \ 0 \le k \le K \end{cases}$$

Figure 3.15 diagrammatically indicates the structure of the principle functions $\psi_i^a(z), \psi_{ij}^b(z)$, and $\psi_{ijk}^c(z)$ as well as how the function $\psi_i^a(z)$ is incorporated into $\psi_{ij}^b(z)$, and similarly how $\psi_{ij}^b(z)$ is incorporated into $\psi_{ijk}^c(z)$. The function $\psi_i^a(z)$ has been decomposed into two linearly varying components and a function which is zero at the end points. This function is identical to the one-dimensional modal expansion which was used in the tensorial construction of the structured modal expansions. The linearly varying components also generate the vertex modes which are identical to the standard linear finite element expansion. The interior contributions of all the base functions (that is, $1 \le i < I, \ 1 \le j < J. \ 1 \le k < K$) are similar to the orthogonal basis functions defined in section 3.2.2. However, they are now pre-multiplied by a factor of the form $\left(\frac{1-z}{2}\right)\left(\frac{1+z}{2}\right)$ which ensures that these modes are zero on the boundaries of the domain. The value of α, β in the Jacobi polynomial $P_p^{\alpha,\beta}(z)$ has also been modified to maintain as much orthogonality as possible in the mass and Laplacian systems. As can be seen in figure 3.15 we have ordered the definition of $\psi^a_i(z), \psi^b_{ij}(z)$, and $\psi^c_{ijk}(z)$ in equations (3.18-3.19) so that the modes can be interpreted according to the physical location of the modes. For example, the vertex modes correspond to the corner location of the arrays. We note, however, that an alternative technique would have been to order the arrays according to increasing polynomial order. Finally we observe that there is a great deal of similarity between $\psi_{ij}^b(z)$ and $\psi_{ijk}^c(z)$. Not only does $\psi_{ijk}^c(z)$ contain $\psi_{ij}^b(z)$ along its boundary but the interior contribution of $\psi_{ijk}^c(z)$ is related to the interior contribution of $\psi_{ij}^b(z)$ since

$$\psi_{ijk}^c(z) = \psi_{i+j,k}^b(z)$$
 $1 \le i, j, k; \ i < I, i+j < J; k < K.$

3.2.3.2 Definition of Expansion Bases

In the same way as the orthogonal expansions, the two-dimensional expansions are defined in terms of the modified principal functions as:

- Quadrilateral expansion: $\phi_{pq}(\xi_1, \xi_2) = \psi_p^a(\xi_1)\psi_q^a(\xi_2)$
 - Triangular expansion: $\phi_{pq}(\xi_1, \xi_2) = \psi_p^a(\eta_1)\psi_{pq}^b(\eta_2)$

where

$$\eta_1 = \frac{2(1+\xi_1)}{(1-\xi_2)} - 1, \quad \eta_2 = \xi_2,$$

are the two-dimensional collapsed coordinates. In figure 3.16 we see all of the modified expansion modes for a fourth-order (P=4) modified triangular expansion. From this figure it is immediately evident that the interior modes have zero support on the boundary of the element. This figure also illustrates that the shape of every boundary mode along a single edge is identical to one of the modes along the other two edges. This was not the case for the orthogonal expansion in section 3.2.2 but is ensured in the modified expansion by the introduction of

Formulation

note: Definition of hierarchical modified C^0 expansions in 2D standard regions.

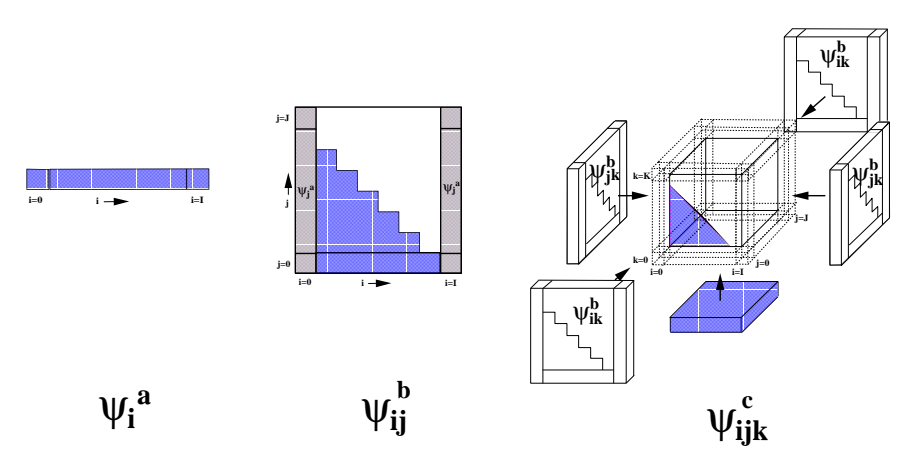


Figure 3.15 Illustration of the structure of the arrays of modified principal functions $\psi_i^a(z), \psi_{ij}^b(z),$ and $\psi_{ijk}^c(z)$. These arrays are not globally close packed although any edge, face, or interior region of the array may be treated as such. The interior of the arrays $\psi_{ij}^b(z)$ and $\psi_{ijk}^c(z)$ have been shaded to indicate the minimum functions required for a complete triangular and tetrahedral expansion.

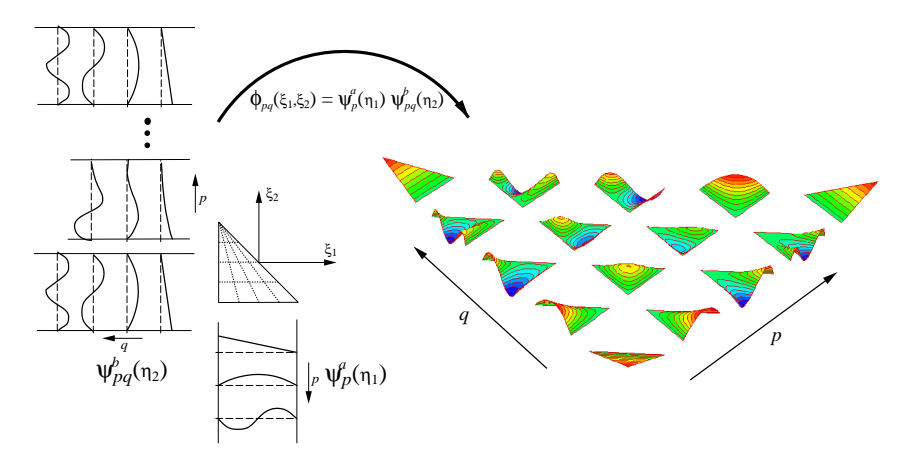


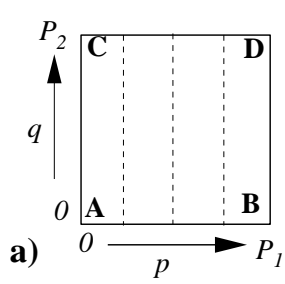
Figure 3.16 Construction of a fourth-order (P=4) triangular expansion using the product of two modified principal functions $\psi_p^a(\eta_1)$ and $\psi_{pq}^b(\eta_2)$. As compared with the orthogonal expansion shown in figure 3.11, the modes are now decomposed into interior and boundary contributions where the boundary modes have similar forms along each edge.

 $\psi_i^a(z)$ into $\psi_{ij}^b(z)$. In the three-dimensional expansion an equivalent condition is ensured by the introduction of $\psi_{ij}^b(z)$ into $\psi_{ijk}^c(z)$. The three-dimensional expansions are defined in terms of the principal func-

tions as:

Formulation

note: Definition of hi $erarchical\ modified\ C^0$ expansions in 3D standard hybrid regions.



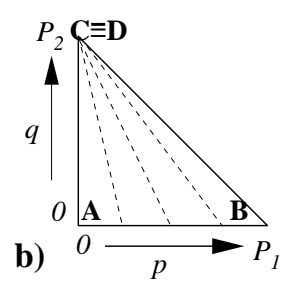


Figure 3.17 The construction of the collapsed Cartesian coordinates system maps vertex D onto vertex C in plot (a). If we consider the quadrilateral region in plot (a) as describing a two-dimensional array in p and q then we can imagine an equivalent array within the triangular region as shown in plot (b).

- Hexahedral expansion: $\phi_{pqr}(\xi_1, \xi_2, \xi_3) = \psi_p^a(\xi_1) \ \psi_q^a(\xi_2) \ \psi_r^a(\xi_3)$
- Prismatic expansion: $\phi_{pqr}(\xi_1, \xi_2, \xi_3) = \psi_p^a(\overline{\eta_1}) \psi_q^a(\xi_2) \psi_{pr}^b(\xi_3)$
- Pyramidic expansion: $\phi_{pqr}(\xi_1, \xi_2, \xi_3) = \psi_p^a(\overline{\eta_1}) \ \psi_q^a(\eta_2) \ \psi_{pqr}^c(\eta_3)$
- Tetrahedral expansion: $\phi_{pqr}(\xi_1, \xi_2, \xi_3) = \psi_p^a(\eta_1) \ \psi_{pq}^b(\eta_2) \ \psi_{pqr}^c(\eta_3)$

where

$$\eta_1 = \frac{2(1+\xi_1)}{(-\xi_2-\xi_3)} - 1, \quad \overline{\eta_1} = \frac{2(1+\xi_1)}{(1-\xi_3)} - 1, \quad \eta_2 = \frac{2(1+\xi_2)}{(1-\xi_3)} - 1, \quad \eta_3 = \xi_3,$$

are the three-dimensional collapsed coordinates.

3.2.3.3 Construction of Modified Basis from Principal Functions

Unlike the structured expansion in the quadrilateral and hexahedral domains, or even the orthogonal expansions introduced in section 3.2.2, the modified principal functions for the unstructured regions are no longer in a close packed form. That is to say, we cannot consecutively loop over the indices p,q, and r. The reason for this is that the introduction of the boundary/interior decomposition destroys the dense packing of the principal functions ψ^b_{pq} and ψ^c_{pqr} , although the indices corresponding to a specific edge, face, or interior modes remain close packed. Even though these arrays are not close packed their definition permits an intuitive construction of the expansion basis by considering each function to be part of an array within the local region.

Two-Dimensional Expansions

Implementation note: Details of how to construct a complete 2D modified basis from principal functions.

In section 3.1, we demonstrated how the quadrilateral expansion may be constructed by considering the definition of the basis $\phi_{pq}(\xi_1, \xi_2)$ as a two-dimensional array within the standard quadrilateral region with the indices p = 0, q = 0 corresponding to the lower left-hand corner as indicated in figure 3.17(a). Using this

diagrammatic form of the array we can construct the vertex and edge modes by determining the indices corresponding to the vertex or edge of interest. A similar approach is possible with the modified triangular expansion.

We recall that to construct the local coordinate system we used a collapsed Cartesian system where vertex D in figure 3.17(a) was collapsed onto vertex C as shown in figure 3.17(b). Therefore, if we use the equivalent array system in the triangular region we can construct our triangular expansions. For example, the vertices marked A and B in figure 3.17(b) are defined as

Vertex A =
$$\phi_{00}(\eta_1, \eta_2) = \psi_0^a(\eta_1)\psi_{00}^b(\eta_2)$$

Vertex B =
$$\phi_{P_10}(\eta_1, \eta_2) = \psi_{P_1}^a(\eta_1)\psi_{P_10}^b(\eta_2)$$
.

The vertex at the position marked CD in figure 3.17(b) was formed by collapsing the vertex D onto vertex C in figure 3.17(a). Therefore, this mode is generated by adding the contribution from the indices corresponding to the vertices C and D, that is,

• Vertex CD =
$$\phi_{0P_2}(\eta_1, \eta_2) + \phi_{P_1P_2}(\eta_1, \eta_2) = \psi_0^a(\eta_1)\psi_{0P_2}^b(\eta_2) + \psi_{P_1}^a(\eta_1)\psi_{P_1P_2}^b(\eta_2)$$
.

From the definition of $\psi^b_{pq}(\eta_2)$ for the modified basis we see that $\psi^b_{0P_2}(\eta_2) = \psi^b_{P_1P_2}(\eta_2)$. This condition was necessary to ensure that all the boundary modes have a similar shape, however, we see that the definition of vertex CD can be simplified to

• Vertex CD =
$$(\psi_0^a(\eta_1) + \psi_{P_1}^a(\eta_1))\psi_{0P_2}^b(\eta_2)$$
.

Finally, recalling the definition of $\psi_n^a(\eta_1)$ we find that

$$\psi_0^a(\eta_1) + \psi_{P_1}^a(\eta_1) = (\frac{1-\eta_1}{2}) + (\frac{1+\eta_1}{2}) = 1$$

and therefore vertex CD is defined as

• Vertex CD =
$$\psi_{0P_2}^b(\eta_2) = (\frac{1+\eta_2}{2}), \quad \left[= (\frac{1+\xi_2}{2}) \right].$$

Although we could have gone straight to this answer, the construction using the analogy of the collapsed coordinate system to the rectangular system is helpful in assembling the three-dimensional basis.

For the triangular expansion the edge modes are defined as:

• Edge AC:
$$\phi_{0q}(\eta_1, \eta_2) = \psi_0^a(\eta_1) \psi_{0q}^b(\eta_2)$$
 $(0 < q < P_2)$

• Edge BD:
$$\phi_{P_1q}(\eta_1, \eta_2) = \psi_{P_1}^a(\eta_1)\psi_{P_1q}^b(\eta_2)$$
 $(0 < q < P_2).$

In constructing the triangular region from the quadrilateral region as shown in figure 3.17, edge CD was eliminated. It does not, therefore, contribute to the triangular expansion.

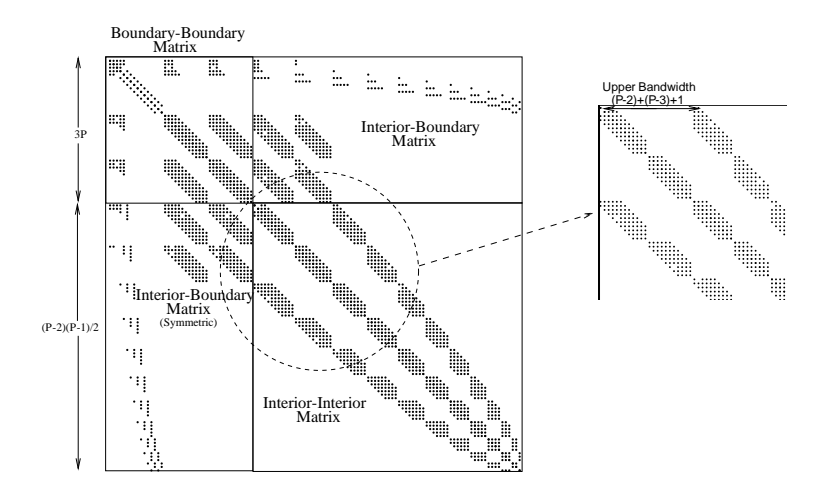


Figure 3.18 The structure of the mass matrix for a triangular expansion $\phi_{pq} = \psi_p^a \psi_{pq}^b$ of order $P_1 = P_2 = 14$ within the standard region \mathcal{T}^2 . The boundary modes have been ordered first followed by the interior modes. If the q index is allowed to run faster, the interior matrix has a bandwidth of (P-2) + (P-3) + 1.

Finally the interior modes of the modified triangular expansion (which become the triangular face modes in the three-dimensional expansions) are defined as

• Interior :
$$\phi_{pq}(\eta_1, \eta_2) = \psi_p^a(\eta_1) \psi_{pq}^b(\eta_2)$$
 $(0 < p, q; p < P_1; p+q < P_2; P_1 \le P_2).$

A full listing of the triangular basis in terms of the Jacobi polynomials can be found in Appendix D. There is a dependence of the interior modes in the p direction on the modes in the q direction which ensures that each mode is a polynomial in terms of the Cartesian coordinates (ξ_1, ξ_2) . This dependence requires that there should be as many modes in the q direction as there are in the p direction, hence the restriction that $P_1 \leq P_2$. A complete polynomial expansion typically involves all the modes defined above and this expansion is optimal in the sense that it spans the widest possible polynomial space in (ξ_1, ξ_2) with the minimum number of modes. More interior or edge modes could be used but if they are not increased in a consistent manner the polynomial space will not be increased. In figure 3.18 we see the structure of the mass matrix for a $P_1 = P_2 = 14$ polynomial order triangular expansion within the standard triangular region. The matrix is ordered so the boundary modes are first followed by the interior system. It can be shown (see [429]) that if we order the interior system so the q index runs fastest then the bandwidth of the interior system is (P-2) + (P-3) + 1.

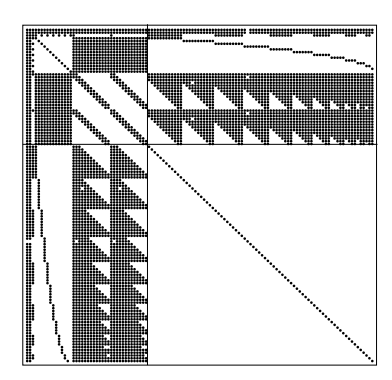


Figure 3.19 The structure of the mass matrix for a triangular expansion of order $P_1 = P_2 = 14$ where the principal function $\psi_i^a(z)$ is defined using $P_i^{2,2}(z)$ and the principle function $\psi_{ij}^b(z)$ is defined using $P_j^{2i+3,2}(z)$. In this case the interior expansion is orthogonal; however, the boundary system has become more dense.

As mentioned previously, the value of α and β in the Jacobi polynomials used in the principal functions $\psi_p^i(z)$ and $\psi_{ij}^b(z)$ were chosen to minimise the bandwidth in both the mass and Laplacian systems. However, as noted by [142, 492] the bandwidth of the interior system of the mass matrix can be made orthogonal by using $P_i^{2,2}(z)$ in the principal function $\psi_i^a(z)$ and $P_j^{2i+3,2}(z)$ in the principal function $P_j^{2i+3,2}(z)$. Nevertheless, as illustrated in figure 3.19 the coupling between the interior and boundary system is stronger.

Three-Dimensional Expansions

As illustrated in figure 3.20, for the hexahedral domain the indices p,q,r correspond directly to a three-dimensional array where all indices start from zero at the bottom left-hand corner. Therefore, the vertex mode labelled A is described by $\phi_{(000)} = \psi_0^a(\xi_1)\psi_0^a(\xi_2)\psi_0^a(\xi_3)$, similarly the vertex mode labelled H is described by $\phi_{(P_1,P_2,P_3)}$, and the edge modes between C and G correspond to $\phi_{0,P_2,r}$ $(1 < r < P_3)$.

Implementation

note: Details of how to construct a complete 3D modified basis from principal functions.

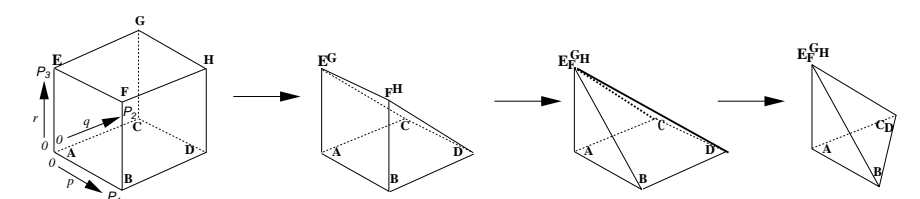


Figure 3.20 Generation of the standard tetrahedral domains from repeated collapsing of a hexahedral region.

When considering the prismatic domain we use the equivalent hexahedral indices. Accordingly, vertex A is now described by $\phi_{(000)} = \psi_0^a(\xi_1)\psi_0^a(\eta_2)\psi_{00}^b(\xi_3)$. In generating the new coordinate system, vertex G was mapped to vertex E and therefore the vertex mode, labelled EG in the prismatic domain, and is described by $\phi_{(0,0,P_3)} + \phi_{(0,P_2,P_3)}$ (that is, adding the two vertices from the hexahedral domain which form the new vertex in the prismatic domain). A similar addition process is necessary for the prismatic edge EG - FH which is constructed by adding the edge modes EF (that is, $\phi_{(p,0,P_3)}$) to the edge modes GH (that is, $\phi_{(p,P_2,P_3)}$). In degenerating from the hexahedral domain to the prismatic region, the edges EG and FH are removed and therefore do not contribute to the prismatic expansion.

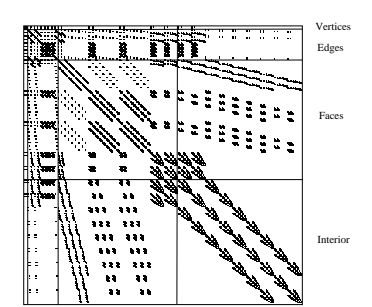
This process can also be extended to construct the expansion for the pyramidic and tetrahedral domains. For both these cases the top vertex is constructed by summing the contribution of E, F, G, and H. In the tetrahedral domain edges CG and DH are also added. Although the modified functions ψ^b_{ij} and ψ^c_{ijk} are not close packed, every individual edge, face, and the interior modes may be summed consecutively. A full listing of all the modes for the hexahedral, prismatic, pyramidic, and tetrahredal expansions is given in Appendix D.

The present construction has assumed that P_1, P_2 , and P_3 have been fixed within the local expansion. In practice, every edge may have a different bound, every face can be described by two bounds, and the interior can be described by three bounds. However, to generate an expansion which spans as complete a polynomial space as possible, all edges which vary with the p index should be assembled from 0 . Similarly, all edges which vary with <math>q or r should be assembled from $0 < q < P_2, 0 < r < P_3$, respectively.

The face modes in all four regions are dependent on the index pairs (p,q), (p,r), and (q,r), where the third index is fixed for a given face. If we let (a,b) represent any one of these three index pairs and P_a, P_b represent the bounds upon which a face is dependent, then the quadrilateral face modes should be assembled over all the indices similar to the edge modes, that is, $0 < a < P_a, 0 < b < P_b$. The triangular faces are dependent upon the function $\psi^b_{ij}(z)$ either directly or indirectly through $\psi^c_{ijk}(z)$. Therefore, the indices for a triangular face are similar to the two-dimensional expansion and should be assembled as $(0 < a, b; a < P_a; a + b < P_b; P_a \le P_b)$.

Finally, the interior assembly depends upon which principal functions are used. In the hexahedral domain, the interior assembly is the same as that used for the edge and quadrilateral faces $(0 . The prismatic domain contains the principal function <math>\psi^b_{qr}(\xi_3)$ and so the interior assembly is similar to the (q,r) face assembly and has the form $(0 . The interior modes for the pyramidic and tetrahedral expansions use the <math>\psi^c_{pqr}(\eta_3)$ principal function and should therefore be assembled up to the limits $(0 < p,q,r; p < P_1; p+q < P_2; p+q+r < P_3; P_1 \le P_2 \le P_3)$.

Providing all the modes used in the each edge, face, and interior assembly are consecutive, then the expansions are complete even though the polynomial space



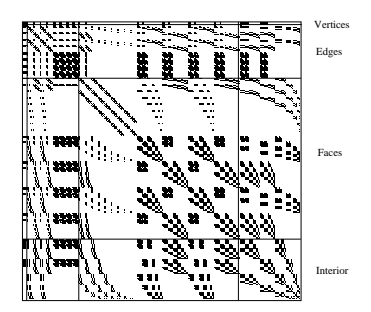


Figure 3.21 Mass matrices for the prismatic (left) and pyramidic (right) domains at a fixed polynomial order of P = 10. Both expansions have been plotted so that the vertex modes are first followed by the edge, face, and finally the interior modes.

of the expansion may not contain as many monomials as the number of modes. With the exception of the pyramidic expansion the above assembly procedure will give polynomial expansions which contain the same number of modes as the monomials in the polynomial space. The pyramidic function does not have this property since boundary/interior decomposition requires that there be a greater number of modes. The pyramidic expansion also differs in the fact that the individual modes are not polynomials in terms of the Cartesian coordinates (ξ_1, ξ_2, ξ_3) . However, the linear combination of the modes does produce an expansion which is complete in terms of polynomials of the Cartesian coordinates.

Although the use of the modified expansion allows the hybrid domains to be tessellated into a global C^0 expansion, this process has reduced the orthogonality of the modes as compared with the orthogonal versions given in section 3.2.2. Nevertheless, the Jacobi polynomials used in the interior of the principal functions $\psi_i^a(z), \psi_{ij}^b(z)$, and $\psi_{ijk}^c(z)$ have been chosen to maintain as much orthogonality in the expansions as possible. To realise this orthogonality the k index must run faster than the j index which must run faster than the i index. Figure 3.21 shows all the non-zero entries of the mass matrix for the prismatic and pyramidic expansion within a single domain using an expansion of polynomial order P=10. A high degree of sparsity is evident particularly in the prismatic region although it should be noted that for a fixed order of $P_1 = P_2 = P_3 = P = 10$ the prismatic expansion has 726 modes whereas the pyramidic expansion has only 386 modes. The structure of the mass matrix for the tetrahedral expansion is also shown in figure 3.22 for polynomial orders of P=4, 9 and P=19.

As a final point we note that the use of the collapsed Cartesian coordinate system means that the coordinate system in the triangular faces, unlike the quadrilateral faces, are not rotationally symmetric. This means that there is a restriction on how two triangular faces, in a multi-domain expansion, must be aligned. In section 4.1.6 we show that this condition can easily be satisfied for all tetrahedral meshes although some care must be taken when using a mixture

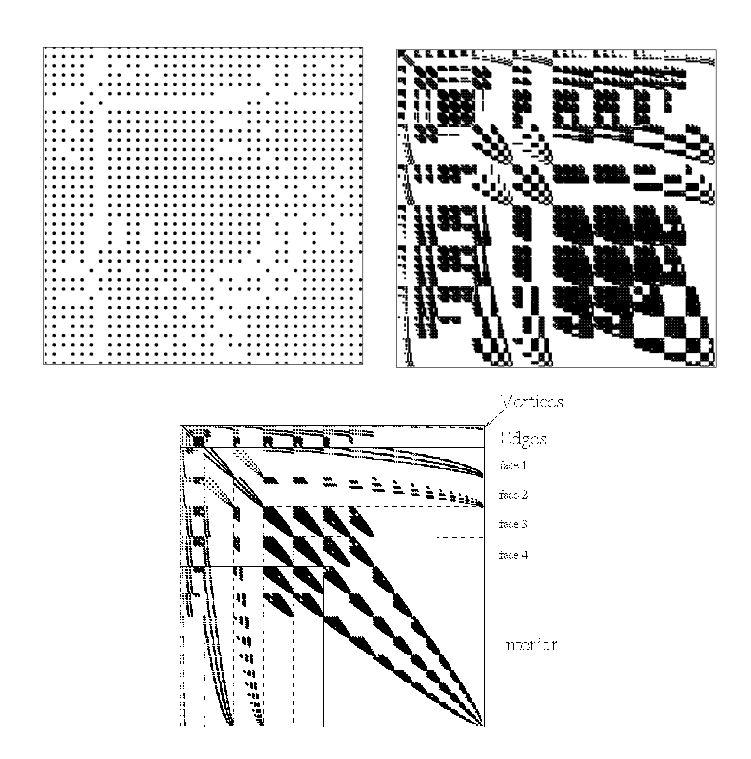


Figure 3.22 The structure of the mass matrix of a tetrahedral expansion in App T^3 for P=4 (top left), P=9 (top right) and P=19 (bottom).

of different elemental domains.

3.2.3.4 Polynomial Space of Modified Unstructured Expansions

The polynomial space of these expansions is the same as the orthogonal expansions [see equation (3.16)], and with the exception of the pyramidic expansion the number of modes is equal to the size of the polynomial space. The pyramidic expansion requires extra modes to perform the interior/boundary decomposition as compared to the orthogonal expansion. Unfortunately, the introduction of these extra modes does not increase the polynomial space of the expansion.

A notable advantage of the boundary/interior decomposition in the modified expansions is the ability to use a different number of modes along every edge, within all faces as well as the interior. Similar to the structured expansions this permits a high level of flexibility in the multi-domain extension where a different polynomial order can be used within every elemental region.

3.3 Non-Tensorial Nodal Expansions in a Simplex

The use of nodal spectral element methods in simplex regions such as triangles and tetrahedrons has also been very limited by comparison to nodal quadrilateral and hexahedral expansions. A nodal type basis was proposed by Mavripilis and Rosendale [323] in 1993 although this has been observed to lead to unstable schemes for P>3 in C^0 continuous spectral elements. A variation of this was discussed in [484] but has not been used widely in any applications. A desirable feature of a nodal triangular basis is that it can be used in conjunction with the standard nodal spectral element. As discussed in sections 2.3.4.2 and 3.1, the nodal spectral element basis commonly uses the tensor product of polynomials through the Gauss-Lobatto-Legendre quadrature points. In this section we shall review two non-tensorial bases within a triangular region, which have edges that match these Gauss-Lobatto-Legendre quadrature points.

Minimisation of Electrostatic Potential

Hesthaven[231] proposed an extension to the concept of using the minimisation of an electrostatic potential (see section 2.3.3.2) to determine a nodal set of points in a triangle. Using the one-dimensional distribution of points to constrain the nodal distribution along the edges, the interior nodal points were then also determined as the minimum of an electrostatic potential. By constraining the edge points in this manner the nodes along all edges can be constrained to the Gauss-Lobatto-Legendre quadrature points. The nodal distribution, therefore, offers a compatible extension to the quadrilateral expansion where both quadrilateral and triangular regions can be assembled into a global C^0 expansion. This expansion has been used in the solution of conservation laws [234], incompressible Navier-Stokes equations [483] and computational electromagnetics [236]. The technique was extended to the tetrahedral region in Hesthaven & Teng [235].

Minimisation of Lebesgue Constant and the Fekete Points

A reasonably good choice for the nodal points within the triangular or tetrahedral region are the points which minimise the Lebesgue constant. The Lebesgue constant is a measure of how close the polynomial approximation to a function is to the best polynomial approximation in the maximum norm. Based on this idea, an alternative to electrostatic minimisation is to search for a nodal set with a small Lebesgue constant by maximising the determinant of the Vandemonde matrix. These points are known as the Fekete points and this basis has been investigated by Bos [69], Chen & Babuška [93] and Taylor, Wingate & Vincent [448]. The last authors applied this nodal basis to computational acoustics in [269]. In one-dimension the Fekete points are also the Gauss-Lobatto-Legendre quadrature points which, as noted previously, are used in the standard quadrilateral spectral element basis. The Fekete distribution is, therefore, a good extension to the nodal quadrilateral expansion. We also note that a nodal distribution of points in a triangle and tetrahedron with an L^2 -norm optimal Lebesgue constant were determined by Chen & Babuška [93, 94] although these points do not have an edge distribution which can be identified with Gauss-Lobatto-Jacobi points.

The nodal basis for a triangular region cannot be defined in terms of a closed form expression, as was the case for the tensorial expansions of sections 3.1 and 3.2. Instead, we define the nodal basis as Lagrange polynomials, denoted as $L_i^{N_m}(\boldsymbol{\xi})$, through a set of Π_{N_m} nodal points in the triangular region where $\boldsymbol{\xi}_i = (\xi_1^i, \xi_2^i)$ and

$$\Pi = \left\{ \boldsymbol{\xi}_0, \boldsymbol{\xi}_1, \dots, \boldsymbol{\xi}_{N_m} \right\}.$$

For the nodal bases to be complete in a linear space of order P, i.e.

$$L_i^{N_m}(\xi) \subseteq \mathcal{P}_P = \operatorname{span} \mathcal{P}_P(\mathcal{T}^2) = \operatorname{span} \{\xi_1^p \ \xi_2^q\}_{(p,q) \in \Upsilon}$$
$$\Upsilon = \{(p,q) | 0 \le p, q; p+q \le P\}$$

then it is necessary that Π_{N_m} must contain (P+1)(P+2)/2 distinct nodal points $\boldsymbol{\xi}_i$.

Since there is not a closed form expression for Lagrange polynomials it is necessary to express the Lagrange basis in terms of another more easily defined polynomial, for example the orthogonal expansion discussed in section 3.2.2. Determining the Lagrange polynomial in terms of another polynomial expansion naturally leads us to the generalised Vandemonde matrix which will be discussed in section 3.3.2. However, before proceeding we recall that a measure of the Lagrange basis through either the electrostatic or Fekete points is through the magnitude of the the Lebesgue constant. Therefore, before introducing the nodal bases we will first discuss the Lebesgue constant in the next section.

3.3.1 The Lagrange Polynomial and Lebesgue Constant

Consider the problem of interpolating a function $f(\boldsymbol{\xi}_i) \equiv f(\xi_1^i, \xi_2^i)$ in the standard triangular region $\Omega_{st} = \mathcal{T}^2 = \{-1 \leq \xi_1, \xi_2; \xi_1 + \xi_2 \leq 0\}$. Given a distinct set of points $\Pi = \{\boldsymbol{\xi}_0, \dots, \boldsymbol{\xi}_{N_m}\}$, we assume a unique polynomial function $g(\boldsymbol{\xi})$ exists which satisfies

$$g(\boldsymbol{\xi}_i) = f(\boldsymbol{\xi}_i) \quad \forall \quad i, 0 \le i < N_m.$$

This polynomial can be considered the interpolating polynomial such that

$$g(\boldsymbol{\xi}) = \mathcal{I}_{N_m} f(\boldsymbol{\xi}),$$

where \mathcal{I}_{N_m} is the interpolation operator. Following [231, 448] the Lebesgue constant shows how well \mathcal{I}_{N_m} approximates $f(\boldsymbol{\xi})$. We denote by $p^*(\boldsymbol{\xi})$ the best approximating polynomial in the max norm, defined as

$$||f||_{\infty} = \max_{\boldsymbol{\xi} \in \Omega_{st}} |f(\boldsymbol{\xi})|.$$

Since $p^*(\boldsymbol{\xi})$ is in the same polynomial space as $\mathcal{I}_{N_m} f(\boldsymbol{\xi})$ we note that $p^* = \mathcal{I}_{N_m} p^*$. Therefore, we observe that

$$||f - \mathcal{I}_{N_m} f||_{\infty} = ||f - p^* + \mathcal{I}_{N_m} p^* - \mathcal{I}_{N_m} f||_{\infty}$$

$$\leq ||f - p^*||_{\infty} + ||\mathcal{I}_{N_m}||_{\infty} ||p^* - f||_{\infty}$$

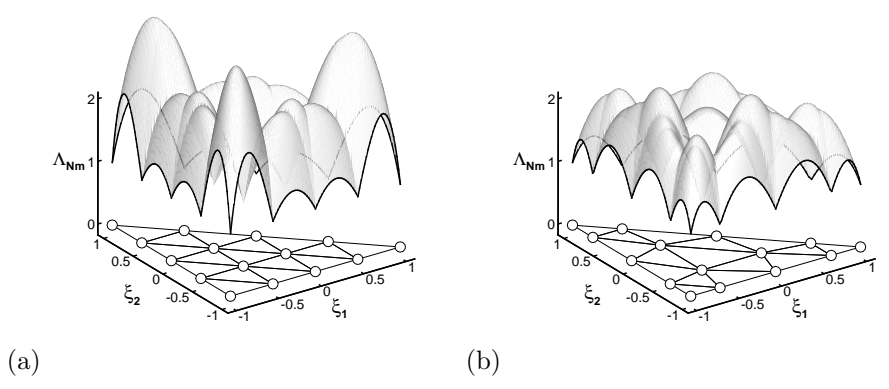


Figure 3.23 Spatial distribution of the Lebesgue function, $\sum_{0 \leq i < N_m} |L_i^{N_m}(\xi)|$, for (a) equispaced points $N_m = 15$, (b) Fekete points $N_m = 15$. The maximum of the Lebesgue function gives the Lebesgue constant Λ_{N_m} . (Courtesy of T.C. Warburton)

$$\leq (1 + ||\mathcal{I}_{N_m}||_{\infty})||p^* - f||_{\infty}$$

where we understand that

$$||\mathcal{I}_{N_m}||_{\infty} = \max_{||f||_{\infty}=1} ||\mathcal{I}_{N_m}f||_{\infty}.$$

The constant $\Lambda_{N_m} = ||\mathcal{I}_{N_m}||_{\infty}$ is known as the *Lebesgue constant*. We observe that the Lebesgue constant is a measure of how close the approximation, $\mathcal{I}_{N_m} f$, is to the best polynomial approximating polynomial p^* in the *max* norm. Choices such as equally spaced points (in the square or triangle) are known to have Lebesgue constants that grow exponentially [448].

If we now represent our polynomial approximation in terms of the Lagrange interpolation or cardinal function at the nodal points, i.e.

$$\mathcal{I}_{N_m}f(oldsymbol{\xi}) = \sum_{i=0}^{N_m} f(oldsymbol{\xi}_i) L_i^{N_m}(oldsymbol{\xi})$$

where

$$L_i^{N_m}(\boldsymbol{\xi}_j) = \delta_{ij}$$

and δ_{ij} is the Kronecker Delta, we observe that

$$\Lambda_{N_m} = ||\mathcal{I}_{N_m}||_{\infty} = \max_{||f||_{\infty} = 1} ||\mathcal{I}_{N_m} f||_{\infty} = \max_{\xi \in \Omega_{st}} \sum_{0 \le i < N_m} |L_i^{N_m}(\xi)|.$$
 (3.21)

Therefore, evaluating the Lagrange polynomials throughout the triangular region, $\boldsymbol{\xi} \in \Omega_{st}$ allows us to get a graphical interpretation of the Lebesgue function, $\sum_{0 \leq i < N_m} |L_i^{N_m}(\boldsymbol{\xi})|$. The maximum bound of this function over the region leads to the Lebesgue constant Λ_{N_m} . The Lebesgue function is illustrated in figure 3.23 where we show plots of $\sum_{0 \leq i < N_m} |L_i^{N_m}(\boldsymbol{\xi})|$ for equispaced and Fekete (see

section 3.3.4) distribution of nodal points when $N_m = 15$ (or P = 4). In this case the equispaced and Fekete points have Lebesgue constants of $\Lambda_{N_m} = 3.47$ and $\Lambda_{N_m} = 2.72$, respectively.

3.3.2 Generalised Vandemonde Matrix

Since there is not a closed form expression for the Lagrange polynomial through an arbitrary set of points in the triangular region it is necessary to express the Lagrange polynomial in terms of another polynomial which has a closed form definition, for example the orthogonal polynomial discussed in section 3.2.2. The choice of the closed form basis is important since ultimately a matrix inversion is involved and therefore the basis dictates the conditioning of the matrix and ultimately the computational stability. Following [483] we consider the interpolation of a polynomial function $p(\xi)$ through a set $\Pi_{N_m} = \{\xi_0, \dots \xi_{N_m-1}\}$ of $N_m = (P+1)(P+2)/2$ distinct points, where P is the polynomial order. The polynomial $p(\xi)$ can be exactly represented by any polynomial expansion, $\phi_i(\xi)$, which spans the same space, i.e.

$$p(\boldsymbol{\xi}) = \sum_{0 \le i < N_m} \phi_i(\boldsymbol{\xi}) \hat{f}_i,$$

where \hat{f}_i represents the expansion coefficients associated with $\phi_i(\boldsymbol{\xi})$. We note that the use of the index i in the above expression denotes a summation over all modes in the expansion. In sections 3.1 and 3.2 we adopted double indices (p,q) to represent a two-dimensional basis constructed from a tensor product of two one-dimensional expansions. We, therefore, understand that a summation over i represents a complete summation over the pair (p,q). Since $p(\boldsymbol{\xi})$ and $\phi_i(\boldsymbol{\xi})$ span the same polynomial space, any form of projection will recover the exact expansion coefficients, \hat{f}_i . We can, therefore, obtain the expansion coefficients by performing a collocation projection at the points $\boldsymbol{\xi}_i$ such that

$$\sum_{0 \leq j < N_m} \phi_j(\boldsymbol{\xi}_i) \hat{f}_j = p(\boldsymbol{\xi}_i) \quad \ \forall \ i, \ 0 \leq i < N_m$$

which can be written in matrix notation as

$$V\hat{f} = f$$

where $f[i] = f(\xi_i)$, $V[i][j] = \phi_j(\xi_i)$ and $\hat{f}[i] = \hat{f}_i$. If $\phi_i(\xi)$ denotes a monomial basis $\phi_i(\xi) = \phi_{i[p,q]}(\xi_1, \xi_2) = \xi_1^p \xi_2^q$ the matrix V is the Vandemonde matrix. For a general basis $\phi_i(\xi)$ the matrix V is known as the generalised Vandemonde matrix. As recognised in [448, 483] the choice of the orthogonal expansion $(\phi_{i[p,q]}(\xi_1, \xi_2) = \psi_p^a(\xi_1)\psi_{pq}^b(\xi_2))$ discussed in section 3.2.2 is particularly convenient due to the strong linear independence of the expansion. This property leads to a well conditioned system which is then amenable to numerical inversion.

A further observation that is worthwhile noting for our subsequent discussion of nodal bases is that when $\phi_p(\boldsymbol{\xi})$ is a known function, such as the orthogonal basis of section 3.2.2, then if $V[i][j] = \phi_j(\boldsymbol{\xi}_i)$ we find that

$$V\begin{bmatrix} L_0(\boldsymbol{\xi}) \\ \vdots \\ L_{N_m-1}(\boldsymbol{\xi}) \end{bmatrix} = \begin{bmatrix} \phi_0(\boldsymbol{\xi}) \\ \vdots \\ \phi_{N_m-1}(\boldsymbol{\xi}) \end{bmatrix} \quad \text{or}$$

$$\begin{bmatrix} L_0(\boldsymbol{\xi}) \\ \vdots \\ L_{N_m-1}(\boldsymbol{\xi}) \end{bmatrix} = V^{-1} \begin{bmatrix} \phi_0(\boldsymbol{\xi}) \\ \vdots \\ \phi_{N_m-1}(\boldsymbol{\xi}) \end{bmatrix} . \tag{3.22}$$

Therefore, given a set of points $\boldsymbol{\xi}_j$ $(0 \leq j < N_m)$ and polynomial functions $\phi_0(\boldsymbol{\xi}), \dots, \phi_{N_m-1}(\boldsymbol{\xi})$ we can evaluate $L_0^{N_m}(\boldsymbol{\xi}), \dots, L_{N_m-1}^{N_m}(\boldsymbol{\xi})$ using equation (3.22). Further details on constructing the generalised Vandemonde matrix can also be found in section 4.1.5.3.

3.3.3 Electrostatic Points

As previously discussed in section 2.3.3.2, Stieltjes [439] and Szego [444] showed the connection between the polynomial $(1-\xi)^{\alpha}(1+\xi)^{\beta}P_{P-1}^{\alpha,\beta}$ and the minimisation of the following problem: Assume that (P-1) unit mass charges with unit charge, are allowed to move freely inside the interval [-1,1] between two fixed unit charges $\alpha \sim \frac{(\alpha+1)}{2}$ and $\beta \sim \frac{(\beta+1)}{2}$ held fixed at $\xi_1 = \pm 1$. The steady state position of the charges that minimises the electrostatic energy:

$$W = -\sum_{i=1}^{P-1} \left\{ \frac{(\alpha+1)}{2} \log |\xi_i + 1| + \frac{(\beta+1)}{2} \log |\xi_i - 1| + \frac{1}{2} \sum_{\substack{j=1\\j \neq i}}^{P-1} \log |\xi_i - \xi_j| \right\}.$$

is the distribution of the Gauss-Lobatto points. An analogous minimisation performed without the two fixed end-charges also leads to the zeros of the Jacobi polynomial $P_{P-1}^{\alpha,\beta}$ or equivalently the Gauss rather then the Gauss-Lobatto quadrature points. Since the Legendre polynomials $L_P(\xi) = P_P^{0,0}(\xi)$ and their derivatives $L'_P(\xi) = \frac{1}{2}(P-1)P_{P-1}^{1,1}(\xi)$ are widely used in both the modal and nodal expansion for quadrilateral and hexahedral domains, Hesthaven [231] adopted a similar approach to that in Stieltjes problem to determine a set of nodal points in the simplex.

As the electrostatic points in one-dimension can be constructed to comply with the Gauss-Lobatto-Jacobi quadrature points, a natural requirement for the distribution of nodes in the triangular region is that the boundary charges are located at these Gauss-Lobatto-Jacobi quadrature points along each edge. In this way it is possible to enforce that the nodal basis is aligned with the quadrilateral nodal basis. Hesthaven [231] assumed the potential from each edge 'e' contributed a potential at a point, ξ , in the triangular region of the form

$$\Psi_e(\xi) = \rho_e \int_0^1 \frac{1}{|\boldsymbol{\xi} - \boldsymbol{\xi}_e|} dt,$$

where $\xi_e = v_a + t(v_b - v_a), t \in [0, 1]$ represents the coordinates along an edge between the vertices v_a and v_b . He then assumed that the N_p unit mass charges were allowed to move mutually interacting according to the potential

$$\Psi(\pmb{\xi}_i, \pmb{\xi}_j) = \frac{\rho_p^2}{|\pmb{\xi}_i - \pmb{\xi}_j|},$$

and posed the following minimisation problem, analogous to that of Stieltjes:

Problem: Let the line charge density be given as $\rho_e > 0$. Assume that N_p unit mass charges with unit charge, $\rho_p = 1$, are allowed to move freely inside the simplex. What is the steady state position of the charges that minimises the electrostatic energy

$$W(\boldsymbol{\xi}_{1},\ldots,\boldsymbol{\xi}_{N_{p}}) = \sum_{i=1}^{N_{p}} \left(\sum_{i=1}^{3} \Psi_{e}(\boldsymbol{\xi}_{i}) + \frac{1}{2} \sum_{\substack{j=1\\j\neq i}}^{N_{p}} \Psi(\boldsymbol{\xi}_{i},\boldsymbol{\xi}_{j}) \right)?$$

In the minimisation the particles were constrained to have certain symmetries motivated by the symmetry of the domain and the likelihood that the optimal points will have strong symmetry. Therefore, the line charge ρ_e was to set the values equal on all edges such that $\rho_1 = \rho_2 = \rho_3$. The value of ρ_e also depended on the choice of Gauss-Lobatto-Jacobi quadrature nodes prescribed on the edges. Therefore, for a symmetrical distribution of edge nodes (i.e., $\alpha = \beta$) there was an additional parameter, α . If $\alpha = -1/2$ the edge points correspond to a Gauss-Lobatto-Chebychev distribution whereas $\alpha = 1$ corresponds to the Gauss-Lobatto-Legendre points commonly used in nodal spectral elements. Finally for a P-order expansion there are $N_p = (\prod)(P+2)/2 - 3P$ points to be determined by the minimisation.

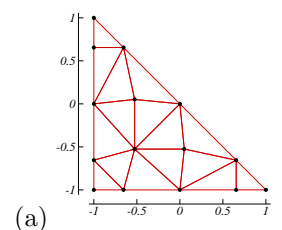
To solve the N_p -body minimisation problem, Hesthaven considered the steady state solution of time-integrating Newton's second law stated as

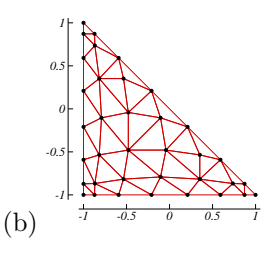
$$m{\xi}_i'' = -\left(\sum_{i=1}^3
abla \xi_e(m{\xi}_i) + rac{1}{2} \sum_{\substack{j=1 \ j
eq i}}^{N_p}
abla \xi(m{\xi}_i, m{\xi}_j)
ight) - \epsilon m{\xi}_i'.$$

The term $\boldsymbol{\xi}_i'$ corresponds to a friction term in order to make the problem slightly dissipative. In solving the problem, highly accurate time integration is required to reduce numerical dissipation, however the value of ϵ does not alter the solution since we are only interested in the steady state solution. The choice of initial conditions is important since finding the global minimum of the energy function

Formulation note: Simplex nodal points

that match the spectral element quadrilateral edge nodes. A full listing of the points is given in appendix D.





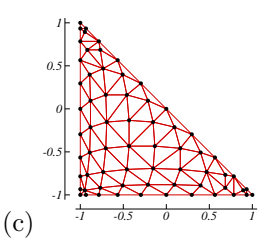


Figure 3.24 Nodal points from electrostatic potential minimisation with the boundary nodes constrained to be the Gauss-Lobatto-Legendre quadrature points at a polynomial order of (a) P = 4, (b) P = 7 and (c) P = 10. (Courtesy of J. Hesthaven)

is particularly complicated, especially for larger N_p . This was partly simplified by imposing a high degree of symmetry onto the nodal location, we refer the reader to [231] for more details.

The distribution of points corresponding to a choice of Gauss-Lobatto-Legendre quadrature distribution on the edges at polynomial orders of P=4,7,10 is shown in figure 3.24, and the values of the Lebesgue constants for these bases are shown in table 3.3. The concept of electrostatic distribution of points has been extended to a tetrahedral domain in the work of Hesthaven & Teng [235], and both the triangular and tetrahedral distribution of points are given in appendix D.

3.3.4 Fekete Points

Following the discussion in section 3.3.1 the optimal distribution of nodal points in a simplex, from the point of view of interpolation, is one which minimises the Lebesgue constant. However, there does not appear to be a feasible method to compute these points. A tractable alternative is to use the Fekete points. Following Taylor et al. [448], Fekete points are a set of points $\Pi_{N_m} = \{\xi_0, \dots, \xi_{N_m}\}$ which maximise (for a fixed basis) the determinant of the Vandemonde matrix, i.e.

$$\max_{\boldsymbol{\xi}_i} |V(\boldsymbol{\xi}_0, \dots, \boldsymbol{\xi}_{N_m})|. \tag{3.23}$$

These points are independent of the choice of basis, since a change of basis only multiplies the determinant by a constant independent of the points.

In the interval [-1, 1], Fejér [156] showed that the Fekete points are the Gauss-Lobatto-Legendre quadrature points. This result was extended to the square and cube by Bos $et\ al.[70]$ who showed that the Fekete points were the tensor product of Gauss-Lobatto-Legendre quadrature points. As discussed in section 3.3.3 the one-dimensional Fekete points are also the minimum energy configuration of the point charges in the interval [439] when the choice of the electrostatic energy contains fixed charges at the end-points. However, in higher dimensions, Fekete points are not Gaussian-like quadrature points or the minimum energy electrostatic points. In the triangular region Bos [69] conjectured that Fekete points contain the one-dimensional Gauss-Lobatto-Legendre point on the boundary and

this was numerically verified in [448]. This is significant since it means that the Fekete points will conform with the quadrilateral spectral elements.

Finally, to understand the connection between the Fekete points and the Lebesgue constant we recall the results of equation (3.22) where the Lagrange polynomial through a set of points $\Pi_{N_m} = \{\boldsymbol{\xi}_0, \dots, \boldsymbol{\xi}_{N_m}\}$ in a triangle can be evaluated as

$$L_i^{N_m}(\boldsymbol{\xi}) = \frac{|V(\boldsymbol{\xi}_0, \dots, \boldsymbol{\xi}_{i-1}, \boldsymbol{\xi}, \boldsymbol{\xi}_{i+1}, \dots, \boldsymbol{\xi}_{N_m-1})|}{|V|}$$
(3.24)

where V is the generalised Vandemonde matrix. By definition of the Fekete points (equation (3.23)) the determinant in the denominator of equation (3.24) is at its maximum value. Therefore, there is no value of $\boldsymbol{\xi}$ in the triangular region that can make the determinant in the numerator larger than the denominator. Only when $\boldsymbol{\xi} = \boldsymbol{\xi}_i$ will the numerator of equation (3.24) equal the denominator, making the Lagrange polynomial equal to one. Therefore, Fekete points generate Lagrange polynomials which achieve their maximum in the triangular region at the associated Fekete point. This property also provides a bound on the Lebesgue constant since from equation (3.21) we observe that when $L_i^{N_m}(\boldsymbol{\xi})$ is evaluated at the Fekete points then

$$\Lambda_{N_m} = \max_{\boldsymbol{\xi} \in \Omega_{st}} \sum_{0 \le i < N_m} |L_i^{N_m}(\boldsymbol{\xi})| \le N_m.$$

In [448] it was numerically observed that the Lebesgue constant using the Fekete points behaved as $C\sqrt{N_m}$. In the one-dimensional case it is also known that the Lebesgue constant behaves as the logarithm of N_m .

3.3.4.1 Evaluation of the Fekete Points

The earliest work on evaluating the Fekete points in a triangle was done by Bos [69] who derived the points up to polynomial order or P=3 and an approximate solution up to P=7. Chen & Babuška [93] improved and extended Bos' results up to P=13. Subsequently, Taylor *et al.* [448] determined the points up to a polynomial order of P=19 with improvement on the numerical points of Chen & Babuška [93] for P>10.

To evaluate the Fekete points, Taylor *et al.* [448] used a steepest ascent algorithm to determine the maximum determinant. This approach solved the ordinary differential system

$$\frac{\partial \boldsymbol{\xi}_i}{\partial t} = \frac{\partial |\boldsymbol{V}|}{\partial \boldsymbol{\xi}_i} \qquad \forall i, \ 0 \le i < N_m$$
 (3.25)

where the points were evaluated by moving their location in the direction of the steepest ascent until an equilibrium was reached, subject to the constraint that the points could not leave the triangular region.

The Fekete point solution presented by Taylor et al. [448] has a very elegant construction and interpretation and we therefore shall revisit it here. Recalling

Polynomial Order, P	Electrostatic points	Fekete points	Equispaced points
6	4.08	4.17	8.45
7	4.77	4.91	14.35
8	5.85	5.90	24.01
9	6.87	6.80	40.92
10	8.44	7.75	70.89
11	10.08	7.89	124.53
12	12.63	8.03	221.41
13	15.34	9.21	397.7
14	22.18	9.72	720.7
15	29.69	9.97	1315.9
16	41.73	12.10	2418.5

Table 3.3 Lebesgue constant Λ_{N_m} (where $N_m = (P+1)(P+2)/2$) for a set of points in the triangular region as a function of polynomial order P for the electrostatic points of Hesthaven [231], the Fekete points of Taylor, Wingate & Vincent [448] and an equispaced distribution in the triangular region. Data was taken from [231, 448] with the permission of the authors.

that we can use any definition of the Vandemonde matrix, V, in equation (3.25), we start by rewriting equation (3.25) as

$$\frac{\partial \boldsymbol{\xi}_{i}}{\partial t} = \frac{\partial |\boldsymbol{V}|}{\partial \boldsymbol{\xi}_{i}} = \sum_{i,j} \frac{\partial |\boldsymbol{V}|}{\partial \boldsymbol{V}_{ij}} \frac{\partial \boldsymbol{V}_{ij}}{\partial \boldsymbol{\xi}_{i}}$$
(3.26)

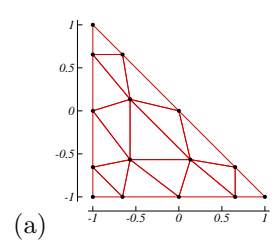
where V_{ij} represents the (i, j) entry of V. We then note that the partial derivative of the determinant of a matrix with respect to an entry V_{ij} is given by

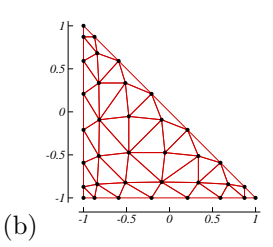
$$\frac{\partial |\mathbf{V}|}{\partial \mathbf{V}_{ij}} = -1^{i+j} |\mathbf{A}_{ij}|,$$

where A_{ij} is the ij minor of V. Now if we choose to define the Vandemonde matrix V with respect to a Lagrange basis the matrix V is the identity matrix. Therefore, the derivative of |V| with respect to any matrix element is only nonzero for diagonal elements. In this case the $i^{\rm th}$ diagonal element is also the $i^{\rm th}$ Lagrange function, $L_i^{N_m}(\boldsymbol{\xi})$, evaluated at the points ξ_i and the determinant of the minor $|A_{ii}| = 1$. Therefore, equation (3.26) becomes

$$\frac{\partial \boldsymbol{\xi}_i}{\partial t} = \frac{\partial L_i^{N_m}}{\partial \boldsymbol{\xi}_i}.$$

The above algorithm has a very simple geometric interpretation which is illustrative of what the Fekete points are trying to achieve in the triangular space. Since we would like the Lagrange functions to approximate a delta function at ξ_i the maximum of the function should be achieved at the nodal point ξ_i . The





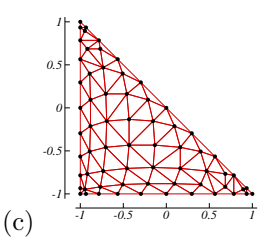


Figure 3.25 Nodal Fekete points at a polynomial order of (a) P = 4, (b) P = 7 and (c) P = 10. (Courtesy of T.C. Warburton)

steepest ascent algorithm simply moves each point towards the maximum of its associated Lagrange function. The iterative nature of the algorithm comes into play because the cardinal functions change with every change in the nodal points and therefore we have to recompute the basis function at every iteration.

To complete the algorithm we also require a technique to evaluate $\frac{\partial L_i^{N_m}}{\partial \boldsymbol{\xi}_i}$. If we denote by \boldsymbol{V}_{ϕ} the Vandemonde matrix between a basis $\phi_i(\boldsymbol{\xi})$ and the Lagrange basis $L_i(\boldsymbol{\xi})$ then differentiating equation (3.22) and evaluating the i^{th} entry we obtain

$$\frac{\partial L_i^{N_m}}{\partial \boldsymbol{\xi}_i}(\boldsymbol{\xi}_i) = \sum_{j=0}^{N_m-1} \boldsymbol{V}_{\phi}^{-1}[i][j] \ \phi_i(\boldsymbol{\xi}_i).$$

Although any basis with a closed form definition is mathematically suitable, numerically it is advantageous to use a basis which is well-conditioned. The orthogonal basis discussed in section 3.2.2 is therefore a good choice and was adopted in [448, 483].

In a similar manner to the electrostatic problem of section 3.3.3 the choice of initial conditions is important. In [448] it was found that the best initial distribution was one which generated a density of points which approximates the extremal measure for a triangle. We refer the reader to [448] for more detail.

In figure 3.25 we show the distribution of Fekete points in a right-handed triangle, the nodal value of which is provided in appendix D. Currently, no points are available for the tetrahedral region. Also shown in table 3.3 are the associated Lebesgue constants of the Lagrange polynomial through the Fekete points. We note that for $P \leq 9$ the electrostatic points have a lower Lebesgue constant but for P > 10 the Fekete points are better with a significant improvement for P > 13 [448].

3.4 Other Useful Tensor Product Extensions

In sections 3.1 and 3.2 we focused on tensor product expansions within standard hybrid regions using either modal or nodal expansion. However, the great power of using a tensor product extension is that we can mix different expansion types according to the problems we are interested in discretising.

Formulation note: Simplex nodal points that match the spectral element quadrilateral edge nodes. A full listing of the points is given in appendix D.

3.4.1 Nodal Elements in a Prismatic Region

In section 2.3.4 we discussed a triangular nodal expansion which is compatible with the standard quadrilateral nodal spectral element discretisation discussed in section 3.1. As we have discussed previously, the quadrilateral expansion $\phi_{pq}^{2D}(\xi_1,\xi_2)=h_p(\xi_1)h_q(\xi_2)$ can be extended to the hexahedral domain by making a tensor product of ϕ_{pq}^{2D} with the Lagrange polynomial in the ξ_3 direction, i.e., $\phi_{pqr}=\phi_{pq}^{2D}(\xi_1,\xi_2)h_r(\xi_3)$. We can perform an analogous extension to the triangular nodal expansions similar to the modal prismatic expansions discussed in 3.2.3. If we denote the triangular nodal expansion as $L_i^{N_m}(\boldsymbol{\xi})=L_i^{N_m}(\xi_1,\xi_2)$, then a prismatic nodal basis which is compatible in terms of nodal location with the hexahedral nodal expansions is $\phi_{pqr}(\xi_1,\xi_2,\xi_3)=L_i^{N_m}(\xi_1,\xi_2)h_r(\xi_3)$.

3.4.2 Expansions in Homogeneous Domains

For a wide range of applications such as flow between parallel plates or past a circular cylinder, the problem of interest contains at least one homogeneous direction. If the homogeneous direction is in the ξ_3 coordinate we can construct a three-dimensional basis $\phi_{pqr}(\xi_1,\xi_2,\xi_3)$ in terms of any two-dimensional expansions discussed previously, denoted by $\phi_{pq}^{2D}(\xi_1,\xi_2)$, multiplied by a complete expansion in ξ_3 , which we shall denote as $\varphi_r(\xi_3)$, that is,

$$\phi_{pqr}(\xi_1, \xi_2, \xi_3) = \phi_{pq}^{2D}(\xi_1, \xi_2)\varphi_r(\xi_3).$$

The above expansion is clearly a tensor product of the two-dimensional basis with the expansion $\varphi_r(\xi_3)$. The absence of any range of scales in the ξ_3 direction encourages us to use a purely spectral, or p-type, expansion which spans the complete homogeneous direction rather than a multi-domain, or h-type, extension.

However, the most convenient choice of $\varphi_r(\xi_3)$ is dependent upon the boundary conditions at the ends of the homogeneous direction. If Dirichlet or Neumann boundary conditions are required at the ends of homogeneous direction then a variety of polynomial expansions might be used including the Legendre polynomial $\widetilde{\psi}_r^a(\xi_3) = L_r(\xi_3)$ or the Chebychev polynomials $T_r(\xi_3) = P_r^{-\frac{1}{2}, -\frac{1}{2}}(\xi_3)$. Each of these expansions have their own desirable properties which are appropriate for a given application (see [197]).

If the domain is periodic in the homogeneous direction then by far the most widely used expansion for $\varphi_r(\xi_3)$ is the Fourier expansion, that is,

$$\varphi_r(\xi_3) = e^{ir\beta\xi_3}$$

where

$$\beta = 2\pi/L_{\xi_3}$$

and L_{ξ_3} is the periodic length. A great attraction of this expansion is the use of Fast Fourier Transform to go between Fourier and physical space. Furthermore, when considering linear differential operators we note that

$$\nabla \phi_{pqr}(\xi_1, \xi_2, \xi_3) = \left[\tilde{\nabla}_r\right] \phi_{pqr}(\xi_1, \xi_2, \xi_3) = \begin{bmatrix} \frac{\partial}{\partial \xi_1} \\ \frac{\partial}{\partial \xi_2} \\ ir\beta \end{bmatrix} \phi_{pqr}(\xi_1, \xi_2, \xi_3),$$

$$\nabla^2 \phi_{pqr}(\xi_1, \xi_2, \xi_3) = \left[\tilde{\nabla}^2_r\right] \phi_{pqr}(\xi_1, \xi_2, \xi_3) = \left(\frac{\partial^2}{\partial \xi_1^2} + \frac{\partial^2}{\partial \xi_2^2} - r^2 \beta^2\right) \phi_{pqr}(\xi_1, \xi_2, \xi_3).$$

The introduction of the operators $\tilde{\nabla}$ and $\tilde{\nabla^2}$ means that we can reduce a three-dimensional linear differential problem to a series of r two-dimensional problems over the Fourier planes. See chapter 9 for details of the application of this expansion to the incompressible Navier-Stokes equations.

3.4.3 Cylindrical Domains

Similar to the Cartesian homogeneous domains, any problem with a rotational symmetry can often be conveniently expressed in cylindrical coordinates. Using cylindrical coordinates allows a Fourier expansion to be imposed in the azimuthal direction which has the favourable properties mentioned in section 3.4.2. However cylindrical coordinates also introduce a radial geometric singularity at the cylinder axis. In solution of the Navier-Stokes system this geometric singularity can be conveniently manipulated by multiplying the equations through by a factor of the radius [348]. Introducing an extra factor of r into the Galerkin framework can lead to a reduction in the convergence rate of the spectral element expansion. For example, Tomboulides et al. [464] and Gerritsma & Phillips [179], have developed a nodal spectral element expansion based on the zeros of the $P_p^{0,1}$ Jacobi polynomials in the radial direction. The two-dimensional expansion is then constructed by a tensor product of the standard Lagrange polynomial through the zeros of the $P_p^{1,1}$ Jacobi polynomial in the axial direction, see [179] for further details. It is, however, also possile to use a standard one-dimensional modal or nodal expansion in the radial direction provided the expansion has a boundary-interior decomposition. As discussed in Blackburn & Sherwin [59] this construction still maintains the exponential convergence of the spectral/hpelement method.

3.5 Exercises: Construction of Multi-Dimensional Elemental Mass Matrices

Building upon the implementation of an one-dimensional spectral/hp element solver presented in chapter 2.6 we begin an analogous multi-dimensional formulation as part of the exercises given in this section. Although there are more formulation and implementation concepts we need to appreciate for a full multi-dimensional, as a starting point we can consider how to numerically construct the multi-dimensional modal and nodal bases. To provide an application for using the multi-dimensional bases we we consider the construction of an elemental mass matrices M^e (see sections 2.3.2.1 and 4.1.5.3) for the different expansion bases. The mass matrix requires the evaluation of the inner product of the modes in an expansion bases with itself, i.e.

$$(\phi_{pq}, \phi_{rs})_{\Omega^e} = \int_{\Omega^e} \phi_{pq}(\xi_1, \xi_2) \phi_{rs}(\xi_1, \xi_2) d\xi_1 d\xi_2.$$

In evaluating the integrals we require some basic integration and numbering concepts which will be introduced in more detail in chapter 4. In section 4.4 we will later provide exercises to extend the elemental matrices into a global matrix and also discuss how to impose boundary conditions. As will also be discussed in last part of section 4.1.5.1, the computation of a mass matrix for a non-tensorial nodal basis can be implemented by considering the Lagrange basis in terms of an orthogonal tensorial expansion. Therefore in the final exercise in this section we will discuss the construction of the generalised Vandemonde matrix which expresses a Lagrange polynomial in terms of another polynomial basis.

Some useful codes are also available on the web page

http://www.ae.ic.ac.uk/staff/sherwin/HpSpectralBook/

1. We start by constructing the elemental mass matrix M^e for a modal quadrilateral expansion $\phi_{pq}(\xi_1,\xi_2)=\psi_p^a(\xi_1)\psi_q^a(\xi_2)$ of order $P_1=P_2=P$ as defined in section 3.1.1. The first part of the implementation is to generate an array containing each component of the tensorial basis, $\psi_p^a(\xi_1)$ and $\psi_q^a(\xi_2)$ at a set of discrete points ξ_{1i},ξ_{2j} . Typically we only require the basis at the discrete quadrature points. Since we have fixed the polynomial order in both expansion directions to P we can also choose to fix the quadrature order in both directions to $Q_1=Q_2=Q$. Depending on the type of Gaussian quadrature adopted we can set Q such that the integration is exact. For example when using Gauss-Lobatto-Legendre integration the choice Q=P+2 will mean each component of the elemental mass matrix is exactly integrated (see section 2.4.1). We now define two arrays base1[p][i], base2[q][j] for $0 \le p, q \le P, 0 \le i, j < Q$ such that

base1[p][i] =
$$\psi_p^a(\xi_{1i})$$

base2[q][j] = $\psi_q^a(\xi_{2j})$

where we recall $\psi_p^a(\xi)$ is dependent upon the Jacobi polynomials defined in appendix A. Code is C and C++ to evaluate the quadrature points and the Jacobi polynomials can also be found on the web page above in the Polylib library. If we are using the same quadrature type, for example Gauss-Lobatto-Legendre (see section 2.4.1.1), in both the ξ_1, ξ_2 directions the arrays base1[p][i] and base2[q][j] will be identical and one array need be defined. Although multi-dimensional integration is discussed in section 4.1.1 we have already seen how it can be applied in one-dimension in section 2.4.1. For the tensor based expansion in a quadrilateral region the product of two one-dimensional integrals, i.e.

$$\mathbf{M}^{e}[n(p,q)][m(r,s)] = \int_{-1}^{1} \int_{-1}^{1} \phi_{pq}(\xi_{1},\xi_{2})\phi_{rs}(\xi_{1},\xi_{2})d\xi_{1} d\xi_{2}$$

Implementation note: Implementation of 2D quadrilateral elemental mass matrices.

$$\begin{split} &= \int_{-1}^{1} \psi_{p}(\xi_{1}) \psi_{r}(\xi_{2}) d\xi_{1} \times \int_{-1}^{1} \psi_{q}(\xi_{2}) \psi_{s}(\xi_{2}) d\xi_{2} \\ &= \left[\sum_{i=0}^{i=Q} w[i] \operatorname{base1}[p][i] \operatorname{base1}[r][i] \right] \times \left[\sum_{j=0}^{j=Q} w[j] \operatorname{base2}[q][j] \operatorname{base2}[s][j] \right] \end{split}$$

where $w[i] = w_i^{0,0}, w[j] = w_j^{0,0}$ are the quadrature weights. In the above operation n(p,q) and m(r,s) denote a mapping from the pair of one-dimensional indices (p,q) and (r,s) in a single unique numbering which represents the location of each two-dimensional mode in the array M^e . There are clearly many different choices of numbering arrays and one of the most straight forward numbering can be constructed as

$$n(p,q) = p \times (P+1) + q, \qquad m(r,s) = r \times (P+1) + s.$$

An alternative numbering scheme would be to place the boundary modes before the interior modes.

(a) To validate your implementation of the two-dimensional Gaussian integration rule, integrate the function $f(x,y)=\xi_1^4\xi_2^5$ in the standard quadrilateral domain using Q=7 points. The function can be numerically evaluated as

$$\int_{-1}^{1} \int_{-1}^{1} \xi_1^4 \xi_2^5 d\xi_1 d\xi_2 = \left[\sum_{i=1}^{i=Q} (\xi_{1i})^4 w[i] \right] \times \left[\sum_{j=1}^{j=Q} (\xi_{2j})^5 w[j] \right].$$

- (b) Construct the two-dimensional mass matrix M^e or rank $N_m = (P + 1)^2$ for P = 7, Q = 9 and plot the structure of the matrix to obtain a similar plot to figure 3.18. Note that in this figure the matrix numbering n(p,q) and m(r,s) has been ordered so that the boundary modes appear first followed by the interior modes.
- (c) Generate the mass matrix M^e for the orthogonal basis $\phi_{pq}(\xi_1, \xi_2) = \widetilde{\psi}_p^a(\xi_1)\widetilde{\psi}_q^a(\xi_2)$ defined in section 3.2.2.1 for P=7, Q=9. Note this is a good debugging exercise since we know it should lead to a diagonal matrix.
- (d) Finally construct the mass matrix for the nodal basis $\phi_{pq}(\xi_1, \xi_2) = h_p(\xi_1)h_q(\xi_2)$ defined in section 3.1.1. In this case the matrix is only "discretely" orthogonal when Q = P + 1. To observe this feature assemble the matrix for P = 7, Q = 9 and P = 7, Q = 8.
- 2. We now consider the construction of the elemental mass matrix for the tensorial based triangular expansion $\phi_{pq}(\xi_1,\xi_2)=\psi_p^a(\eta_1)\psi_{pq}^b(\eta_2)$ defined in 3.2.3.1. In general, this follows a very similar construction to the quadrilateral case but we now need to use the collapsed coordinate system defined in section 3.2.1.1. As will be discussed in more detail in section 4.1.1.2,

Implementation note: Implementation of 2D triangular elemental mass matrices. the integration of the basis ϕ_{pq} over the triangular region $\Omega_{st} = \mathcal{T}^2 = \{(\xi_1, \xi_2) | -1 \leq \xi_1, \xi_2; \ \xi_1 + \xi_2 \leq 0\}$ can be expressed as

$$\mathbf{M}^{e}[n(p,q)][m(r,s)] = \int_{-1}^{1} \int_{-1}^{-\xi_{1}} \phi_{pq}(\xi_{1},\xi_{2}) \phi_{rs}(\xi_{1},\xi_{2}) d\xi_{1} d\xi_{2}
= \int_{-1}^{1} \int_{-1}^{1} \psi_{p}^{a}(\eta_{1}) \psi_{pq}^{b}(\eta_{2}) \psi_{r}^{a}(\eta_{1}) \psi_{rs}^{b}(\eta_{2}) \left(\frac{1-\xi_{2}}{2}\right) d\eta_{1} d\eta_{2}
= \int_{-1}^{1} \psi_{p}^{a}(\eta_{1}) \psi_{r}^{a}(\eta_{1}) d\eta_{1} \int_{-1}^{1} \psi_{pq}^{b}(\eta_{2}) \psi_{rs}^{b}(\eta_{2}) \left(\frac{1-\xi_{2}}{2}\right) d\eta_{2}$$

where

$$\eta_1 = \frac{2(1+\xi_1)}{(1-\xi_2)} - 1, \qquad \eta_2 = \xi_2.$$

Once again we observe that a generalised tensor product basis can be evaluated as two one-dimensional type integrals. We can also use different types of Gauss-Jacobi quadrature which automatically absorb the factor of $\left(\frac{1-\xi_2}{2}\right)$ into the quadrature weights (see section 4.1.1.2). The zeros and weight which contain this factor are denoted as $\xi_i^{1,0}$ and $w_i^{1,0}$ and can also be generate using the Polylib library available on the web page. To continue the construction of the mass matrix we define two arrays base1[p][i], base2[p][q][j] for $0 \le p, q \le P, 0 \le i, j < Q$ such that

$$\begin{split} \text{base1}]p][i] &= \psi^a_p(\xi^{0,0}_{1i}) \\ \text{base2}[p]]q][j] &= \psi^b_{pq}(\xi^{1,0}_{2j}) \end{split}$$

where $\psi_p^a(\xi)$ and $\psi_{pq}^b(\xi)$ depend upon Jacobi polynomials defined in appendix A and can be numerically determined using the Polylib library. As discussed in section 3.2.3.1 the array base2[p][q][i] does not have to contain all entries since only some components are required to evaluate the full bases $\phi_{pq}(\xi_1,\xi_2)=\psi_p^a(\eta_1)\psi_{pq}^b(\eta_2)$. Having constructed base1[p][i] and base2[p][q][j] we can discretely construct the mass matrix as

$$\begin{split} \boldsymbol{M}^{e}[n(p,q)][m(r,s)] &= \int_{-1}^{1} \psi_{p}^{a}(\eta_{1}) \psi_{r}^{a}(\eta_{1}) \ d\eta_{1} \int_{-1}^{1} \psi_{pq}^{b}(\eta_{2}) \psi_{rs}^{b}(\eta_{2}) \left(\frac{1-\xi_{2}}{2}\right) \ d\eta_{2} \\ &= \sum_{i=0}^{i=Q} w_{1}[i] \ \mathrm{base1}[p][i] \mathrm{base1}[r][i] \\ &\times \sum_{j=0}^{j=Q} w_{2}[j] \ \mathrm{base2}[p][q][i] \ \mathrm{base2}[r][s][i], \end{split}$$

where $w_1[i] = w_i^{0,0}, w_2[j] = w_j^{1,0}/2$. Unlike the quadrilateral expansion, for this case the index array n(p,q), m(r,s) cannot be defined in close packed

form. This point is discussed in section 4.1.5.1 and highlighted in figure 4.6. As also discussed in section 3.2.3.3 special attention must be taken when constructing the top vertex which is decomposed into two contributions from the base [p][q][j].

- (a) Construct the two-dimensional mass matrix M^e or rank $N_m = (P + 1)(P+2)/2$ for P=14, Q=16 and plot the structure of the matrix to recover figure 3.18. Recall that in this figure the matrix numbering n(p,q) and m(r,s) has been ordered so that the boundary modes appear first followed by the interior modes. The indices q and s must run faster than the indices p and r to observe the semi-orthogonal structure of the matrix.
- (b) Construct the two-dimensional mass matrix \mathbf{M}^e for the orthogonal triangular expansion $\phi_{pq}(\xi_1, \xi_2) = \widetilde{\psi}^a_p(\eta_1)\widetilde{\psi}^b_{pq}(\eta_2)$ and verify that your matrix is diagonal.
- 3. In this final exercise we will consider how to construct the Lagrange polynomial $L_i^{N_m}(\boldsymbol{\xi})$ through a set of nodal points $\boldsymbol{\xi}_i = [\xi_{1i}, \xi_{2i}]^T$ using the orthogonal triangular tensorial basis $\phi_{pq}(\boldsymbol{\xi}) = \widetilde{\psi}_p^a(\xi_1)\widetilde{\psi}_{pq}^b(\xi_2)$. From section 3.3.2 we recall that the Lagrange polynomial can be evaluated using the generalised Vandemonde matrix \boldsymbol{V} as

$$\begin{bmatrix} L_0(\boldsymbol{\xi}) \\ \vdots \\ L_{N_m-1}(\boldsymbol{\xi}) \end{bmatrix} = \boldsymbol{V}^{-1} \begin{bmatrix} \phi_0(\boldsymbol{\xi}) \\ \vdots \\ \phi_{N_m-1}(\boldsymbol{\xi}) \end{bmatrix}. \tag{3.27}$$

Whilst we can use any polynomial expansion which spans the same polynomial space as $L_i^{N_m}$, the choice of the orthogonal expansion leads to a well conditioned generalised Vandemonde matrix which is important for numerical inversion. For a discrete set of nodal points ξ_i , $0 \le i \le N_m$ through which we define the Lagrange polynomial we can construct the generalised Vandemonde matrix

$$V[m(p,q)][i] = \widetilde{\psi}_p^a(\eta_{1i})\widetilde{\psi}_{pq}^b(\eta_{2i})$$

where

$$\eta_{1i} = \frac{2(1+\xi_{i1})}{1-\xi_{2i}}, \quad \eta_{2i} = \xi_{2i}$$

and m(p,q) denotes a mapping between the index pair (p,q) and the unique index m, for example

$$m(pq) = q + \frac{p(2P+1-p)}{2}.$$

Inverting V, for example using a LAPACK [13], we can then evaluate the Lagrange polynomials $\mathcal{L}_{i}^{N_{m}}(\boldsymbol{\xi})$ at any desired location, $\boldsymbol{\xi}$, using equation (3.27).

(a) Determine the P=4 order Lagrange polynomial expansion using $N_m=(P+1)(P+2)/2=15$ modes through a set of equispaced points

$$\xi_{1i} = \frac{2i}{P+1} - 1, \ \xi_{2j} = \frac{2j}{P+1} - 1, \quad 0 \le i, j; i+j \le (P+1)$$

To plot the function evaluate the Lagrange polynomials, $L_i^{N_m}$, using equation (3.27) and evaluate the Lagrange functions at P=8 ($N_m=45$) equispaced points.

- (b) Determine the P=4 order Lagrange polynomial expansion using $N_m=15$ modes through the electrostatic points defined in appendix D and evaluate the Lagrange functions at P=8 ($N_m=45$) equispaced points.
- (c) Evaluate the Lebesgue function $\sum_{0 \leq i < N_m} |L_i^{N_m}(\boldsymbol{\xi})|$ for the Lagrange polynomial defined at equispaced and electrostatic nodal points for P=4 and compare your function to figure 3.23.